Advanced Drug Delivery Reviews 143 (2019) 22–36

Contents lists available at ScienceDirect

Advanced Drug Delivery Reviews

journal homepage: www.elsevier.com/locate/addr

Ligand density on nanoparticles: A parameter with critical impact on nanomedicine

Alaaldin M. Alkilany [a,b,*], Lin Zhu [a], Horst Weller [c], Alf Mews [c], Wolfgang J. Parak [a,c,d], Matthias Barz [e], Neus Feliu [a,**]

[a] Fachbereich Physik and CHyN, Universität Hamburg, Hamburg, Germany
[b] Department of Pharmaceutics & Pharmaceutical Technology, School of Pharmacy, The University of Jordan, Amman 11942, Jordan
[c] Fachbereich Chemie, Universität Hamburg, Hamburg, Germany
[d] CIC Biomagune, San Sebastian, Spain
[e] Institut für Organische Chemie, Johannes Gutenberg-Universität Mainz, Mainz, Germany

ARTICLE INFO

Article history:
Received 10 December 2018
Received in revised form 25 April 2019
Accepted 29 May 2019
Available online 31 May 2019

Keywords:
Nanotechnology
Nanoscience
Nanoparticles
Antibody
Targeting
Ligand density

ABSTRACT

Nanoparticles modified with ligands for specific targeting towards receptors expressed on the surface of target cells are discussed in literature towards improved delivery strategies. In such concepts the ligand density on the surface of the nanoparticles plays an important role. How many ligands *per* nanoparticle are best for the most efficient delivery? Importantly, this number may be different for *in vitro* and *in vivo* scenarios. In this review first viruses as "biological" nanoparticles are analyzed towards their ligand density, which is then compared to the ligand density of engineered nanoparticles. Then, experiments are reviewed in which *in vitro* and *in vivo* nanoparticle delivery has been analyzed in terms of ligand density. These results help to understand which ligand densities should be attempted for better targeting. Finally synthetic methods for controlling the ligand density of nanoparticles are described.

Contents

1. Introduction: from passive to active targeting

Nanotechnology is recognized as a research area with the potential to improve a wide range of biomedical applications [1]. From a pharmaceutical perspective, nanotechnology offers tools to improve solubility and stability of pharmaceutical active ingredients (APIs) and thus enhancing bioavailability. Moreover, nanotechnology can become a powerful tool to alter the pharmacokinetics and biodistribution of APIs (the topic of this review falls in this category). From a clinical

* Corresponding author at: Department of Pharmaceutics & Pharmaceutical Technology, School of Pharmacy, The University of Jordan, Amman 11942, Jordan.
** Corresponding author at: Fachbereich Physik and CHyN, Universität Hamburg, Hamburg, Germany.
E-mail addresses: a.alkilany@ju.edu.jo (A.M. Alkilany), nfeliu@physnet.uni-hamburg.de (N. Feliu).

https://doi.org/10.1016/j.addr.2019.05.010
0169-409X/

perspective, the driving force to develop nanomedicine is to improve efficacy, reduce toxicity, improve patient compliance, or enable completely novel therapeutic interventions. The number of food and drug administration (FDA) approved nanotechnology medicines and devices is constantly increasing. Currently, there are >50 products in clinical practice and many others under clinical evaluation [2–5].

The first FDA approved drug delivery system is Doxil® (1995) [6], a doxorubicin containing liposomal drug delivery system that utilizes the enhanced retention and permeation effect (EPR), which was first observed by Hiroshi Maeda (1986) [7], to improve accumulation of the anticancer doxorubicin into solid tumors and to minimize doxorubicin related cardiotoxicity which limits its maximum tolerated dose (MTD). The first generation of doxorubicin containing liposomes was based on simple phospholipids and thus exhibited a short plasma half-life and a fast clearance by the reticuloendothelial system (RES) [6]. The second generation was engineered by employing polyethylene glycol (PEG)-ylated lipids to add stealth characteristics and minimize opsonization and RES clearance [6]. The benefit of nanotechnology in the case of Doxil® originates from the "EPR-mediated passive targeting" and thus it is typically indicated in tumors where EPR effect is efficient due to good blood perfusion [8]. In another example, the driving force to develop Abraxane® (A FDA approved formulation of paclitaxel bound to albumin nanoparticles) was the extreme poor aqueous solubility of paclitaxel and the need to replace the toxic cremophor EL® (a solubility enhancer in the original formulation of Taxol®). However, it was realized that paclitaxel bound to albumin nanoparticles (about 150 nm size) has superior pharmacokinetics and tumor sequestration capability compared to free paclitaxel due to the EPR-mediated passive targeting [9–12].

Beside the discussed approved nanomedicines that can make profit of EPR-mediated passive targeting, only a few FDA approved nanomedicines can home to the desired target passively (no targeting ligands) but *via* different mechanism. For example, AmBisome® are a liposomal formulation of the antiprotozoal drug amphotericin B, which has a serious nephrotoxicity [2,13]. Since amphotericin B is used to treat Leishmania (for which macrophages of spleen and liver serve as safe havens), a non-PEGylation choice is preferred to intentionally allow fast RES clearance of AmBisome® by macrophages, the desired target, resulting in significantly lowered nephrotoxicity and superior MTD and clinical outcome [13]. This targeting is passive but not achieved *via* the classical EPR-mediated passive targeting, but indeed, it is a RES-mediated passive targeting [14,15]. Another approved nanomedicine that benefits from the RES-mediated passive targeting are iron oxide nanoparticles to treat iron deficiency anemia (in products such as Feraheme®, Venofer®, and Fereinject®), which are neither PEGylated nor functionalized with targeting moieties but rather they exhibit fast RES uptake and accumulate in the macrophages. Accumulation of iron oxide nanoparticles in macrophages is advantageous and allows sustained release of iron ions into plasma upon gradual dissolution of the nanoparticle cores. Table 1 summarizes approved nanotherapeutics that home to their targets passively with no targeting moieties.

The discussed "success stories" above highlight the fact that passive targeting (EPR or RES-mediated) can be a powerful tool to improve pharmacokinetics and target accumulation. Over the last decades, scientists realized, however, that the EPR effect is highly variable between preclinical models and can differ largely even in patients with the same kind of cancer [16]. A critical analysis surveying the literature from the past 10 years found that only 0.7% (median) of the administered nanoparticle dose is found to reach solid tumors [17], which highlights a poor targeting to tumors and underlines the associated complexity of nanomedicines [18].

In this context and considering the early notation "There's Plenty of Room at the Bottom, Richard Feynman", which fueled the field of nanotechnology, it is widely accepted that "active targeting" will be naturally the next leap of nanomedicine [19,20]. For example, recent studies have been shown that when tumor targeting ligand (iRGD) was conjugated or co-administered with Abraxane®, the efficacy of the therapy was improved by several folds in animal models [21]. Up to date, no nanomedicine is approved with targeting ligands (active targeting).

The term active targeting refers to a ligand mediated receptor interaction, which can lead to binding to a cell surface or endocytosis facilitating target cell accumulation. The involved ligands can be antibodies, homing peptides, nucleic acids, aptamers, and small molecules, which can be attached to the surface of nanoparticles [22]. In addition to nanoparticles' size, shape, curvature, elasticity, surface charge, *etc.*, which are heavily evaluated parameters affecting cellular uptake, biodistribution, pharmacokinetics and toxicity of non-targeted nanoparticles, ligand

Table 1
Summary of nanotherapeutics approved by FDA (U·S food and drug administration) or EMEA (European medicines agency) which home to their cellular targets or tumor tissue by passive mechanism with no targeting moieties. Data obtained from USFDA and EMEA websites and New Drug Application (NDA) numbers for FDA or Agency product numbers for EMEA approved products are provided for reference.

	Product name	Nanoparticle type/active ingredient	Indication	Approved by	New Drug Application (NDA) number for FDA or Agency product number for EMEA approved products
1	Doxil	Liposomal doxorubicin	HIV-related Kaposi sarcoma, ovarian cancer, and multiple myeloma	FDA	50718
2	Marqibo	Liposomal vincristine	Acute lymphoblastic leukemia	FDA	202497
3	Onivyde	Liposomal irinotecan	Post-gemcitabine metastatic pancreatic cancer	FDA	207793
4	DaunoXome	Liposomal daunorubicin	HIV-related Kaposi sarcoma	FDA	50704
5	Myocet	Liposomal doxorubicin	Metastatic breast cancer	EMEA	EMEA/H/C/000297
6	Mepact	Liposomal muramyl tripeptide phosphatidylethanolamine	Nonmetastatic, resectable osteosarcoma	EMEA	EMEA/H/C/000802
7	Vyxeos	liposmal Cytarabine and Daunorubicin	Acute myeloid leukemia	FDA	209401
8	Abelcet	Liposomal amphotericin B	Antifungual for treatment of viscular leishmaniasis	FDA	050724
9	AmBisome	Liposomal amphotericin B	Antifungual for treatment of viscular leishmaniasis	FDA	50740
10	Visudyne	Liposomal verteporfin	Subfoveal choroidal neovascularization	FDA	21119
11	Diprivan	Liposomal propofol	Sedation or anesthesia	FDA	19627
12	Curosurf	Liposomal proctant alfa	Respiratory Distress Syndrome	FDA	20744
13	Abraxane	albumin bound paclitaxel	Breast, lung and pancreatic cancer	FDA	21660
14	Venofer	Iron sucrose colloid	Iron replacement for anemia treatment in patients with chronic kidney disease	FDA	21135
15	Feraheme	Ferumoxytol (iron-based colloid)	Iron deficiency in patients with chronic kidney diseas and recently as an imaging agent to predict EPR and nanotherapeutic response	FDA	22180

type, conjugation strategy, orientation, and ligand density are of critical importance for targeted nanoparticles [23]. While the global evaluation of targeted nanoparticles and bioconjugation chemistries is discussed in recent reviews [22,24–34], this review focuses on the effects of ligand density on targeted nanoparticles as a critical but often overlooked parameter. In this section, we have briefly discussed the importance of active targeting. In the next sections we will focus on the ligand density starting by a brief comparison between the ligand density on natural bionanoparticles (viruses) and on their counterparts, engineered nanoparticles. Next, we will discuss available reports that evaluated the effect of ligand density on the biological behavior of nanoparticles *in vitro* and *in vivo*. Finally, we wrap up with a description of the available chemistries to control the ligand density on nanoparticles.

2. Ligand density on targeted nanoparticle: comparison between natural and engineered counterparts

The idea of adding targeting moieties to nanoparticles originates from lessons learned from nature, as many cellular uptake mechanisms of small molecules and bionanoparticles are mediated *via* specific and selective antigen-receptor recognition. For example, viruses are small bionanoparticles of 30–100 nm in diameter, which invade cells by attachment of viral spikes to receptors on host cells (wide array of cell surface molecules of proteins, lipids and glycans) to propagate infection. The virus binding is typically highly specific with low intrinsic affinity, and thus viruses usually bind to multiple receptors, which add multivalent character to the total binding and enhance binding avidity and subsequently induce trans-bilayer signaling and initiate endocytosis or trigger membrane fusion [35]. Learning from nature, and since the early 1980s [36], scientists realized that decorating engineered nanoparticles with targeting moieties is an appealing approach to facilitate their binding and homing into a desired biological destination. An interesting question in this context is how the ligand density of engineered nanoparticles compares to the one on viruses? Despite the difficulty of answering this question, we tried to compile available quantitative data regarding the number of ligands on viruses (spikes) and compare it to the number of targeting ligands on engineered nanoparticles using reported values.

Spikes density on viruses depends on the type of virus. Current data suggests a spike density on the surface of viruses on the order of 1 spike per 100 nm^2 (for example, the Influenza virus of 100 nm in diameter has around 450 spikes) [37]. Compilation of available data on the surface spike density of a number of viruses is shown in Table 2 [37]. As these spikes are responsible for cellular attachment/uptake and at the same time they are the primary targets for host antibodies, the spike density is highly regulated and a general notation implies that viruses must work out an optimized spike density to achieve a fine balance to evade host immunity and to exhibit an optimized cellular infectivity [38]. For example, the human immunodeficiency virus (HIV) exhibits an exceptionally low spike density (0.01 spikes per 100 nm^2, which is two orders of magnitude less than the mean spike density for other viruses) that helps the virus to delay the production of neutralizing antibodies against it [39]. It should be noted here that research showed that low spike density is sufficient to achieve infection, albeit at low efficiency, while increasing spike density significantly enhances infectivity until a plateau is reached, indicating that only a fraction of spikes is required for efficient infection [40,41]. Moreover, spikes on HIV are mobile in the virus envelope and can form clusters when in contact with T cells, compensating the low density and facilitating cellular entry [42]. In another example, it has been shown that increased glycoproteins on Ebola viruses (which promote viral attachment/fusion to host cell and at the same time are the primary target for host neutralizing antibodies) impair their infectivity [38].

Regarding ligand density on engineered nanoparticles, compiled values of the quantified targeting ligand density in available reports in which the implication of ligand density on cellular uptake and systemic biodistribution was studied are summarized in Table 2. They are compared with reported values of viral spike densities in Fig. 1. Interestingly, we noticed that the ligand density of nanoparticles is often reported qualitatively as “low, intermediate and high”, or as a percentage from maximum. Few reports quantitatively determine the number of ligands per nanoparticle. Nonetheless, examination of Table 2 suggests a higher ligand density on engineered nanoparticles compared to viruses (range 0.17–83 ligand per 100 nm^2 of nanoparticle surface). Moreover, a recent review compiled reported values of (non-targeted) ligand densities on inorganic nanoparticles with a mean of 357 ligand per 100 nm^2 (95% confidence interval of 276–439 ligands per 100 nm^2) [43]. Even for large proteins such as albumin (65,000 Da), the reported ligand density on gold nanoparticles was quantified to be 3 and 13 in two independent reports using different quantification methodologies [43]. Collectively and learning from nature, it is apparent that nanoscientists usually employ “more than required” ligand density for targeting that nature does not strictly follow to optimize cellular infectivity while smartly avoiding immune systems. With this in mind, optimizing ligand density on nanoparticles using lessons learned from nature sounds essential and an appealing approach.

Herein, central questions would be: What is the optimum ligand density on engineered nanoparticle? To which extent does the optimal density depend on the ligand itself and other nanoparticle-related parameters (*e.g.* size, shape and charge)? What is the penalty of deviating from this optimum? How can we control the ligand density on engineered nanoparticles? The following sections/discussion attempt to address these questions.

At high ligand density, the probability of binding should increase by the rules of polyvalency and avidity, and thus we should expect

Table 2
Summary of reported values of spike density on various types of viruses compared to reported ligand density on engineered nanoparticles.

Virus type	Diameter (nm)	Spike number per virus	Surface spike density (spikes per 100 nm^2)	Reference
Human immunodeficiency virus (HIV)	120	7–14	0.01	[39,44]
Zika	60	60	0.53	[45]
Herpes Simplex Virus	186	659	0.6	[46]
Influenza A	120	450	1	[47]
Dengue	41	60	1.13	[48]
Hepatitis C virus (HCV)	73	290	1.73	[49]
Nanoparticle type	**Diameter (nm)**	**Targeting ligand**	**Surface ligand density (ligands per 100 nm^2) (up to)**	**Reference**
Nanographene oxide (nGO)	50 nm	Folate	19	[50]
Hydrogel PRINT nanoparticles	80 × 320 nm and 55 × 60 nm	EGFR binding antibody	0.45	[51]
Superparamagnetic iron oxide	26 nm	HER2/neu targeting affibodies	1.7	[52]
gold nanoparticle (GNP)	40 nm	RGD	83	[53]
PLGA based nanoparticles (PLGA-b-PEG-b-Apt)	160 nm	A10 aptamer	0.17	[54]

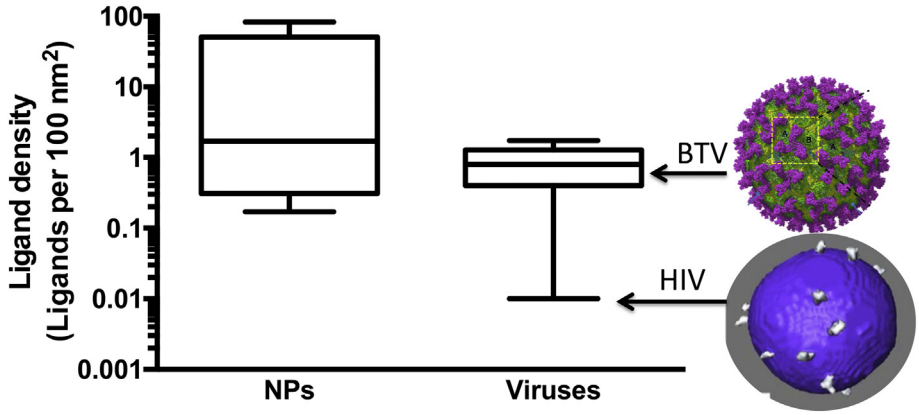

Fig. 1. Spikes density on viruses *versus* ligand density on engineered nanoparticles. BTV: blue tongue virus. Data are a graphical presentation of entries from Table 2. HIV and BTV images are used by permission of Nature publishing Group from reference [55] and reference [56], respectively.

enhanced binding of nanoparticles to the target. However, the penalty associated with high ligand density includes: 1) decreased stealth character of nanoparticles as a result of decreased surface presentation of antifouling molecules (such as PEG) at elevated presentation of targeting moieties, which ultimately initiates opsonization cascade and RES clearance form systemic circulation, 2) increased hydrodynamic diameter of nanoparticles, which deteriorates accumulation in tumor *via* the EPR effect, 3) decreased diffusion coefficient of targeted nanoparticles in tumor tissue, 4) steric hindrance of closely packed ligand that may inversely deteriorate binding of nanoparticles to target, 5) consumption of high number of cell membrane receptors/targets which decreases the overall cellular uptake.

These penalties are summarized in Fig. 2. In the following sections, we examine available reports investigating the effect of ligand density on engineered nanoparticles, both *in vitro* and *in vivo*.

3. Optimum ligand density: *in vitro* studies

It is well accepted that targeted nanoparticles may exhibit superior cellar binding compared to their non-targeted counterparts [54,57–59]. Our questions in this section are: How does the ligand density on the surface of nanoparticles affect the interaction of targeted nanoparticles with cells? Is there an optimum density of targeting ligand at the cellular level?

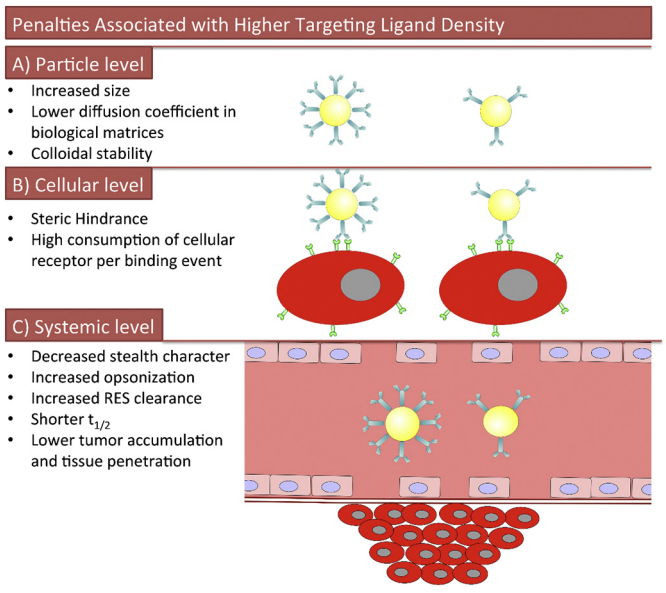

Fig. 2. Penalties associated with higher ligand density on engineered nanoparticles at the nanoparticle, cellular, and systemic level.

Examination of available *in vitro* studies unveils a general trend. When the ligand density increases, the cellular association increases as well to a limit, after which a constant or decreased association is observed. We term the first trend as "optimum density with a plateau", and the later as "optimum density with maximum". Both trends are shown in Fig. 3. Definitely, and when *in vivo* studies and clinical evaluation is the main concern, the definition should be the minimum amount of targeting moieties that guarantee maximum clinical outcome.

Moreover, we noticed that in many published reports the number of nanoparticles which entered the cells is quantified without differentiating the amount bound just to the outer membrane of the cells from the amount which got effectively into the cells [60]. Therefore, we use here the term "cellular association" as the sum of the two different but related events: 1) cellular binding and 2) cellular internalization. Internalization, not simply binding, is for several nanotherapeutics a critical requisite to achieve therapeutic efficiencies. Despite the importance of quantitative deconvolution of these two events this is frequently overlooked in many available reports.

In one report, carful deconvolution of "cellular binding" and "cellular internalization" of rod-shaped targeted nanoparticles revealed an interesting dependence of these events from the ligand density [51]. As the ligand density increased, the authors observed an increased fraction of nanoparticles bound to their targets on the cell membrane. However, the fraction of nanoparticles which entered cells increased only up to a point when ligand density increased, after which a decrease was observed, *i.e.* "optimum density with a maximum". These observations were explained by the large contact area of the rod-shaped nanoparticles (80 × 320 nm) with the cell, which may deplete available receptors to fully wrap the nanoparticles by cell membrane, and therefore, endocytosis is decreased. It is very important to note here that the same report documented very different behavior when spherical targeted nanoparticles were evaluated (50 nm) [51]. For the later, increasing ligand density had very minimal effect on the fraction of bound or internalized nanoparticles. The authors explained this behavior by the size being close to 50 nm, which is considered as the optimal size for cellular uptake, and thus the ligand density has minimal contribution on cellular internalization [51]. The significant difference in cellular association, binding, and internalization between the two nanoparticles that have the same composition, type of targeting ligand, and conjugation strategy calls for considering a serious interplay between ligand density and other parameters such as nanoparticle size (in this case) as well as shape, surface charge., *etc.* [51] In another study, superparamagnetic iron oxide (SPIO) nanoparticles labeled with HER2/neu targeting affibodies at intermediate ligand density provided statistically significant improvement in cell binding in comparison to higher and lower ligand densities

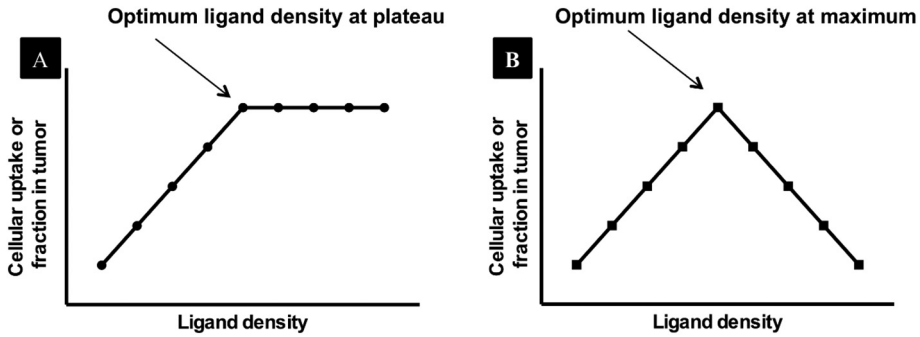

Fig. 3. Reported trends of cellular uptake or tumor homing of engineered nanoparticles as function of ligand density.

(optimum ligand density with maximum). The authors further confirmed that this intermediate optimal ligand density was conserved across nanoparticles with different size (26 and 50 nm, both spherical) and also when the nanoparticles were labeled with small targeting molecule (namely folic acid) [52]. The authors did explain their observation by two possible factors: 1) high density of ligands may results in consuming high numbers of receptors per nanoparticle, which may result in diminished receptor availability for other nanoparticles to bind and enter the cell; 2) tight packing of ligands on the nanoparticle surface results in "steric hindrance", which can decrease the overall recognition and antigen-receptor binding and ultimately impair effective cellular uptake. Using a mathematical model, Ghaghada *et. al* concluded that cellular uptake of targeted liposomes increases with an increase in the number of ligands per liposome until the number of ligands per liposome reaches approximately 500, beyond which a decrease in liposome uptake was observed [61]. The decrease in liposomal uptake at high ligand density was explained by the limited internalization/externalization rates of folate receptors, which controls the entry of folate bound liposomes into cells. This mathematical modeling is supported by independent *in vitro* and *in vivo* studies in which folate targeted liposomes yielded the highest binding activity to folate-expressing cells *in vitro* and transfection activity *in vivo* at optimum ligand density with maximum [62]. However, folate-mediated targeting has to be investigated with great care, since upon conjugation folic acid is rather hydrophobic and can induce aggregation itself [63]. Therefore, these physicochemical effects may also need to be considered, when optimal density of ligands is discussed.

We would like to mention that the conjugation strategies in the discussed reports so far were site-directed conjugation that allows orientated assembly of antibodies on the surface of nanoparticles. With this in mind, one expects that a high density of ligand should induce steric hindrance and over-crowding effects (may prevent closely-packed ligands to adapt the proper orientation for binding). These effects are amplified when crowded ligands have the same orientation. However, when ligand conjugation is not oriented but rather random (*e.g.* using 1-ethyl-3-(3-dimethylaminopropyl)carbodiimide (EDC) coupling chemistry or electrostatic adsorption), optimum ligand density with maxima may not be observed and instead optimum ligand density with plateau may operate. In non-oriented conjugation, antibodies which are lying on their side may act as a "spatial filler" to keep a distance between properly oriented ligands as sketched in Fig. 4, which decrease the steric hindrance effect and ensure effective binding. In support to this notation, the DeSimone group reported that increasing the ligand density of transferrin on polymeric nanoparticles (non-oriented conjugation) from 0 to 25% resulted in increased cellular uptake which plateau afterward and no further increase was observed at 100% (saturation) ligand density [64]. To examine the effect of the ligand density on the nuclear transport of quantum dots (QDs) Warren Chan's group varied the ligand densities of nuclear localization signal (NLS) peptides [65]. A space filler peptide (a random peptide sequence that showed no nuclear transport activity) was used to maintain a constant surface density of total peptides. The authors showed a drastic and linear increase in nuclear transport with NLS densities up to 20%, with only a modest increase in nuclear transport at higher NLS density (optimum density with a plateau). As the used conjugation was oriented on these QDs *via* poly-histidine-Zn ion interaction, the co-use of "filler control" peptide perhaps minimized the crowding effect and thus no "optimum ligand density with maximum" was observed. Optimum density with a plateau was also observed for poly(lactic-*co*-glycolic acid) (PLGA) nanoparticles that were made by co-assembly of a tunable ratio of PLGA-PEG and PLGA-PEG-aptamer (PEG was considered as a spatial filler between PEG-aptamer brushes) [54]. The interplay between the effect of the ligand density and the strategy of conjugation adds to the overall complexity when considering variables related to targeted nanoparticles. This may explain, in part, the conflicting results in the literature regarding the effect of ligand density on the biological behavior of nanoparticles when different conjugation strategies were employed.

In addition to the impact of ligand density on nanoparticle quantitative association and uptake in to cells, it can alter the uptake mechanism by cells and the intracellular trafficking significantly.

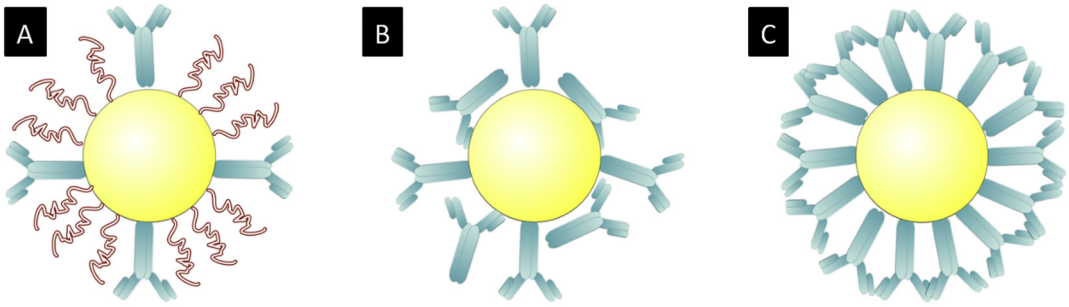

Fig. 4. Effect of conjugation strategy on "steric hindrance" between oriented antibodies. In all cases, the nanoparticles' surface is saturated and "maximum antibody density" is theoretically assumed. In (A) an oriented conjugation with filler (such as PEG) results in less steric hindrance between antibodies. In (B) non-oriented conjugation is employed where non-oriented antibodies reduce steric hindrance between oriented antibodies. In (C), oriented conjugation without filler was employed, where closely packed antibodies may suffer from sever steric hindrance. Theoretically, the penalty of overcrowded antibodies and steric hindrance is more dominant when oriented conjugation is used at high density.

For example it has been shown that the mechanism of uptake for polymer coated quantum dots (35–50 nm) is highly dependent on the folate ligand density. As the folate density shifts from low to intermediate to high, the uptake was operated by caveolae-mediated, mixed, or chathrin-mediated endocytosis, respectively [66]. In another report the mechanism of cellular uptake and intracellular trafficking of liposomes modified with different densities of the octaarginine peptide was studied at low and high ligand densities [67]. Authors found that liposomes modified with a low peptide density are taken up mainly through clathrin-mediated endocytosis, leading to extensive lysosomal degradation, while those modified with a high peptide density were taken up mainly through macropinocytosis, and were less subject to lysosomal degradation. This significant shift in the intracellular trafficking is highly important when considering nanoformulations to deliver sensitive cargo such as genetic materials or proteins that are sensitive to lysosomal degradation and can benefit from avoiding this deteriorating fate by switching uptake mechanisms and intracellular trafficking [67]. It is worth to mention that the effect of ligand density on cellular uptake, potential lysosomal escape, and intracellular trafficking should be considered case by case as it was found to be dependent on the type of evaluated cells as well as the type of targeting moiety [68,69].

4. Optimum ligand density: *in vivo* studies

Simpler and faster *in vitro* studies (in comparison to *in vivo* studies) serve as a preliminary surrogate to evaluate the contribution of targeting moiety-related attributes such as selectivity, specificity, bioactivity, orientation, presentation, and density. However, *in vivo* systems are much more complex and thus call for much higher demands for efficient targeting. For reaching the desired target, nanoparticles need to overcome physiological barriers and need to avoid opsonization and RES clearance. In general, active targeting can take place when ligands on the nanoparticle and receptors are in close proximity to each other. Therefore, one can argue that active and passive targeting are linked to each other. Passive accumulation, like the EPR effect, brings nanoparticles into tumor nodes, but most importantly the nanoparticles need to deeply penetrate the dense tumor tissue to reach the majority of tumor cells. Tumor penetration is hindered by a high interstitial pressure and poor vasculature in the deep center of the tumor [70–72]. For thorough discussion on these physiological barriers that occur *in vivo* (opsonization/RES clearance, interstitial pressures and diffusion into tumor tissue), excellent reviews are available [19,70,71,73–76]. With this in mind, it is critically important to understand the contribution of ligand density on targeted nanoparticles *in vivo*.

To minimize inter-report variability, in the following discussion we will focus on reports evaluating the effect of ligand density using both, *in vitro* and *in vivo* settings and the same: 1) nanoparticles, 2) targeting ligand, 3) conjugation strategy, and 4) quantification approaches (head-to-head comparison). A summary is given in Table 3. In one study, the ligand density (of tripeptide Arg-Gly-Asp, RGD) on targeted nanoparticles with the ability to reduce bleeding was evaluated both *in vitro* and *in vivo*. A 100-fold increase in the surface density of targeting peptide resulted in 10-fold increase efficacy *in vitro* and 8 fold increase in survival rate *in vivo*. In this report only two levels of ligand density were evaluated, low and high, and thus an optimum density cannot be determined. It is worth to mention that authors observed that increased ligand density enhanced the potency of these nanoparticles and at the same time increased adverse effects at high doses both, *in vitro* and *in vivo* [77]. However, the degree of RES uptake as function of ligand density was not clear.

In another report, it was shown that the cellular uptake of nano grapheneoxide (nGO) by KB cells increased steadily with the increase in ligand density (folate) *in vitro*. In contrast, upon intravenous administration into KB tumor-bearing mice similar steady increase in tumor targeting by increasing ligand density was not observed. The authors found that tumor accumulation of nGO did not show a significant targeting effect up to 25% of ligand coating density with a strong and comparable tumor accumulation of nGO for both, 50% and 100% ligand density (optimum ligand density with plateau) [50].

Farokhzad's group prepared self-assembled nanoparticles functionalized with PEG and an aptamer that binds to the prostate-specific membrane antigen on the surface of prostate cancer cells [54]. The authors controlled the density of PEG and aptamer on the surface of the nanoparticle by mixing various ratio of PLGA-b-PEG and PLGA-b-PEG-b-Apt triblock copolymers. They found that increasing the aptamer density on the nanoparticle surface increases the rate of nanoparticle uptake by cells *in vitro* until a plateau was reached (Fig. 5A). However, at high aptamer surface density (beyond the optimum maximum as shown in Fig. 5B) a decrease in tumor targeting and an increase in liver and spleen accumulation were observed. The authors explained this important difference between *in vitro* and *in vivo* based on the masking effect of aptamer that reduces the presentation of PEG brushes on the nanoparticle surface, thus decreasing the nanoparticle antibiofouling charter (stealth properties) *in vivo*, resulting in significant RES clearance. These results call for optimizing a proper balance between targeting and antibiofouling moieties in engineering targeted nanoparticles to achieve optimum targeting efficiency [54].

A straightforward method for the synthesis of colloidal nanoparticles functionalized with a discrete number of antibody molecules with a precise control on the ligand density on each nanoparticle has been developed [78]. For example, gold nanoparticles were synthesized with exactly one or two antibodies (trastuzumab) and then the *in vitro* and *in vivo* behavior of both conjugates was studied. The *in vitro* results showed no significant difference in cellular labeling between nanoparticles labeled with one or two antibodies (Fig. 5C). However, cytotoxic effects were moderately higher when two antibodies were conjugated to the nanoparticles. On the other hand, *in vivo* targeting was clearly improved for nanoparticles conjugated with one antibody *versus* nanoparticles conjugated with two antibodies (Fig. 5D). Moreover, renal clearance was more efficient for nanoparticles conjugated with only one antibody with a lower fraction accumulating in liver and spleen. The results might be explained with the hypothesis that the smaller size of nanoparticles with one antibody makes the combined actions of the EPR effect and active targeting more effective ass compared to nanoparticles functionalized with two antibodies. This would suggest that at high ligand density, the penalties due to an increase in the overall size of nanoparticles in the form of decreased accumulation into tumor *via* the passive targeting and increased RES uptake, may not get compensated by the moderately enhanced targeting at the cellular level. Phrases slightly differently, increased RES uptake due to the presence of two instead of one antibody per nanoparticle decreases the circulation half-life in blood, which simply reduces the chance of a nanoparticle to reach the tumor by the EPR effect.

It is well accepted that increasing ligand density on the nanoparticle alters their biodistribution and pharmacokinetics compared as to non-targeted nanoparticles. It has been shown that nanoparticles targeted with EGFR affibodies have dramatically different biodistribution parameters as compared to non-targeted PEGylated counterparts with a direct correlation to ligand density. For example, the circulation half-life decreased from 11.2 h with the PEG control to 3.9, 3.3, and 0.7 h with increasing ligand density (low, intermediate and high, respectively) [51]. Even with the decreased circulation half-life, tumor accumulation improved as a function of ligand density, indicating possible multivalent effects towards the high epidermal growth factor receptor (EGFR)-expressing cells in tumor. It is interesting to mention that PEGylated nanoparticles without any targeting ligands accumulated in the tumor statistically more than targeted nanoparticles with high ligand density for rod-shaped (80×320 nm) nanoparticles, but similarly in the case of smaller spherical nanoparticles (55×60 nm) (due to longer circulation time). These observations further highlight the direct interplay between active and passive targeting at one hand and the ligand density

Table 3
Summary of available reports evaluating the *in vitro* and *in vivo* outcome of engineered nanoparticles as function of ligand density.

Nanoparticle type	Shape	Dimensions (nm)	Targeting ligand	*In vitro* outcome	*In vivo* outcome	Reference
Gold nanoparticles (GNP)	Spherical	40	RGD	Ligand density affected cellular uptake and adipogenic differentiation of human mesenchymal stem cells	Not conducted in this study	[53]
QDs (polymer coated)	Spherical	35–50	Folate	Cellular uptake mechanism has been shifted as function of ligand density (at low, intermediate and high density, caveolae-mediated, mixed or chathrin-mediated endocytosis was the predominant mechanism of nanoparticle entry to cells, respectively)	Not conducted in this study	[66]
QDs	Spherical	4.5	NLS targeting peptide	Cellular uptake and nuclear accumulation of nanoparticles depend on the surface density of the nuclear localization signal (NLS) peptides with nuclear transport reaching a plateau at 20% surface NLS density "Optimum density with plateau"	Not conducted in this study	[65]
SPIONs	Spherical	26 and 50	— HER2/neu targeting affibodies — Folate molecules	For both ligand and nanoparticle sizes, intermediate ligand density improves cell binding compared to higher and lower ligand densities.	Not conducted in this study	[52]
PEG-based nanoparticles	Cylindrical	200 × 200; height × diameter	— Antibody targeting transferrin — Human Transferrin	Cellular uptake and toxicity of nanoparticles increased with ligand surface density "Optimum density with plateau"		Not conducted in this study [64]
PLGA-based nanoparticles	Spherical	160	Aptamer	Cellular uptake of nanoparticles increased with ligand surface density "Optimum density with plateau"		[54]
Nanographene oxide	Single atom thick, two-dimensional sheets	50	Folic acid	Cellular uptake of nGO by KB cells increased steadily with the increase in ligand density	The *in vivo* experiment in mouse xenograft model did not show the steady increase in tumor targeting by increasing ligand density. Upon intravenous administration into KB tumor-bearing mice, tumor accumulation of nGO did not show a significant targeting effect up to 25% of ligand coating density. However, a strong and similar tumor accumulation of nGO was observed for both 50% and 100% folate coatings.	[50]
Hydrogel nanoparticles	Rod-shaped and spherical	80 nm × 320 and 55 nm × 60 nm	EGFR binding affibody	The 55 × 60 nm type displayed cellular association independent of ligand density while 80 nm × 320 showed an optimum density with maxima (increase cellular uptake up to maximum after which a decreases observed)	Both nanoparticle sizes experienced significant changes in biodistribution and pharmacokinetics as a function of ligand density	[51]
PLGA based nanoparticle	Spherical	500	RGD	Increasing the targeting peptide concentration 100-fold increased the *in vitro* efficacy 10-fold	Increasing the targeting peptide concentration by 100-fold increased the efficacy of nanoparticles by 8-fold	[77]

and nanoparticle size at the other hand, which may explain conflicting results in the literature. Collectively, it is clear that the ligand density has a profound effect on nanoparticles' *in vivo* behavior including pharmacokinetic parameters and tumor homing efficiency.

5. The interplay between ligand density and other parameters

While recent efforts to understand the effect of ligand density on nanoparticles' biological fate are increasing, little is done so far to evaluate how the ligand density contribution is dependent on nanoparticles' properties such as size, shape, surface charge and others. It is highly expected that the ligand density interplays with other nanoparticle-related and experiment-related parameters as shown in part in the previous sections. In this section we discuss published reports in which the interplay between ligand density and another parameter(s) was evaluated, which should enrich our understanding in the effect of ligand density in the big picture and layout knowledge-based fundamentals to engineer smarter nanotherapeutics.

As discussed in the previous sections, the DeSimone group evaluated the effect of ligand density on cellular uptake and tumor targeting using two types of nanoparticles: sphere-like (55 × 60 nm) and rod-shaped (80 × 320 nm) nanoparticles functionalized with EGFR binding affibodies [51]. Interestingly, *in vitro* studies showed that increasing the ligand density improved cellular association of targeted cells at the highest ligand density only for the rod-shaped (80 × 320 nm) but not for the spherical (55 × 60 nm) hydrogel nanoparticles. Remarkably, by quantitatively unraveling the amount of nanoparticles bound to cell membrane and the amount of nanoparticles entered into cells, the authors concluded that the increased cellular association in the case of the rod-shaped nanoparticles is originating from increased binding to cell membrane and not due to more internalization into cells. In fact, as the ligand density for the rod-shaped nanoparticles increased, the nanoparticle fraction which had entered cells decreased as shown in Fig. 6A. The observed results were explained by a receptor-depletion mechanism and thus limited receptor-mediated endocytosis (rod-shaped nanoparticles decorated at high ligand density are competing for receptors, and due to the large contact area of the rod-shaped nanoparticles with cells, there is a depletion of available receptors to fully wrap the nanoparticles by the cell membrane, and therefore, uptake is decreased). The 55 × 60 nm nanoparticles,

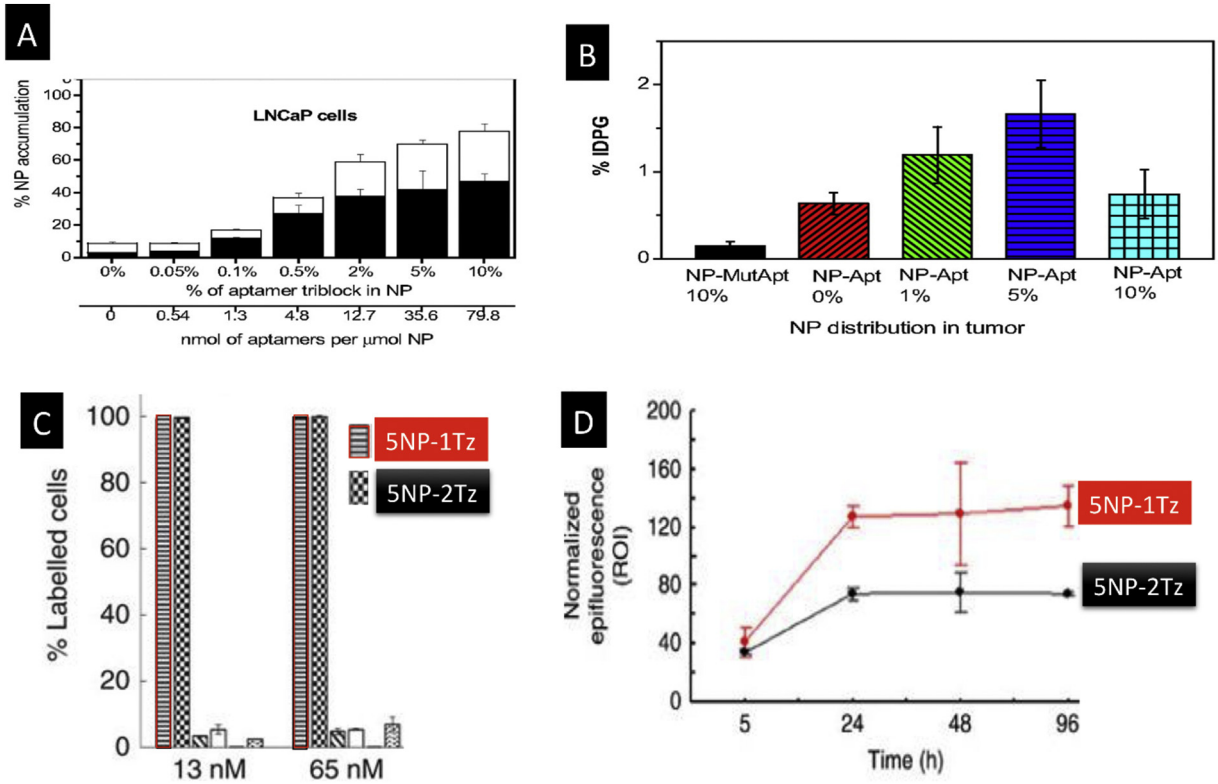

Fig. 5. Two examples show how the effect of ligand density may differ in both, *in vitro* and *in vivo* settings. Upper panel: Cellular uptake of PLGA nanoparticles functionalized with 0–10% aptamer in (A) compared to tumor targeting *in vivo* expressed as % of injected dose per gram (% IDPG) in (B). Note that *in vitro* evaluation suggested an optimum ligand density with plateau whereas *in vivo* evaluation suggested optimum ligand density with maximum. Lower panel: Gold nanoparticles (5 nm) with one (5NP-1Tz) or two (5NP-2Tz) trastuzumab antibodies were compared *in vitro* (C) and *in vivo* (D). While there is no significant difference in cellular uptake for both nanoparticles (shown in C as percent labeled cells at two concentrations, 13 and 65 nM), a clear significant difference in tumor accumulation was found with higher tumor homing for 5NP-1Tz. Graphs in (A) and (B) are reused by permission of National Academy of Sciences from reference [54]. Graphs in (C) and (D) are reused by permission of Nature publishing Group from reference [78].

however, displayed cellular association independent of ligand density, which was explained by their size being optimum for cellular uptake (50 nm) and thus insensitive to the ligand density effect (Fig. 6B). These two nanoparticles showed also very different behavior *in vivo* as function of ligand density as discussed in previous sections. This example is of special importance, since it shows how ligand density effects are highly dependent on nanoparticle size and shape [51]. This interplay is also important to consider when comparing reports using different experimental settings and definitely to design efficient nanotherapeutics.

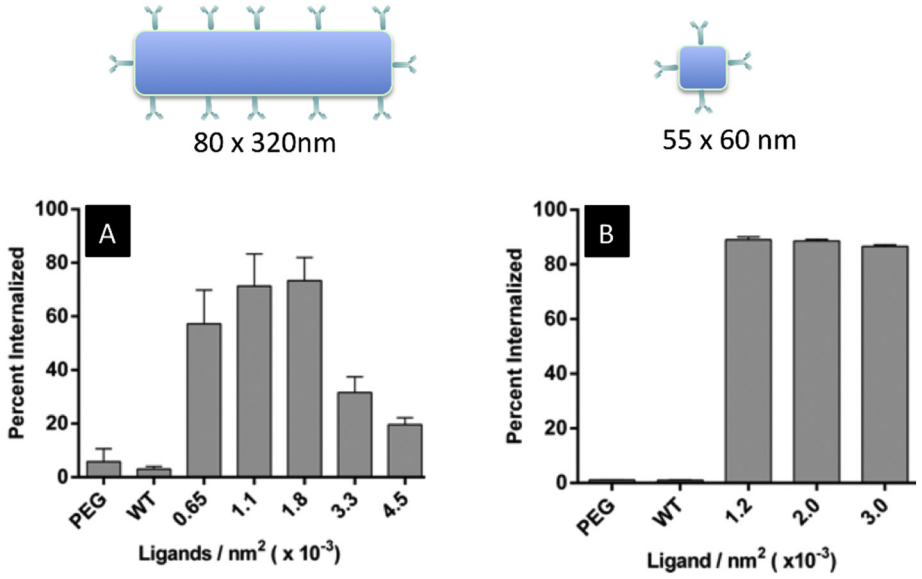

Fig. 6. Interplay between ligand density of targeting moiety on engineered nanoparticles and nanoparticles' size and shape. Cellular uptake of rod-shape (A) or spherical (B) polymeric nanoparticles functionalized with EGFR binding affibody. PEGylated and wild-type functionalized nanoparticles were used as negative controls (labeled as PEG and WT, respectively in the graphs). Graphs in (A) and (B) are reused by permission of American Chemical Society from refereecne [51].

Barua *et. al* reported the effect of nanoparticles' shape (spheres, rods and discs) on cellular binding and uptake of targeted polystyrene nanoparticles at comparable ligand density (trastuzumab) [79]. They found that rod-shapes polystyrene nanoparticles exhibit the highest, where spherical nanoparticles exhibit the lowest cellular association, because the former intrinsically provide a higher surface to volume ratio. The observed improved binding, specificity, and cellular uptake of trastuzumab-targeted rods were explained by the high surface area per unit volume and due to the flat nature of the rods, which increases contact area with the receptors on cell membranes and promotes superior multivalent interactions. Indeed, important theoretical modeling and simulations highlighted the importance of nanoparticles' size, shape, curvature, and length of spacer in determining the probability of adhesion of targeted nanoparticle to cellular receptors [80–86,87].

Another parameter that has a potential interplay with ligand density is the "spatial presentation" of targeting ligands on the surface of nanoparticles. For example, it has been shown that mixed micelles presenting folate ligands as "patchy clusters" have different cellular association compared to the same mixed micelles presenting the same total number of folate molecules that are homogenously distributed overall the micellar surface [88]. Interestingly, a clear dependence of the cellular association and tumor homing on the size of these clusters was observed (optimum cellular and tumor uptake was achieved when cluster had 3 folate molecules per cluster at the reported experimental settings: micelle size = 80–90 nm, total folate molecules per micelle = 2000–2400, evaluated cluster size range = 1.5–16.5 folate molecules/cluster) [88]. Similar enhancement of cellular association was observed by another group when albumin functionalized with folate and "naked" albumin were *co*-assembled on polystyrene nanoparticles to prepare nanoparticles with clustered folate molecules [89]. These examples highlight the importance of considering the "spatial presentation or clustering effect" of targeting ligands in addition to the "global density of targeting moiety" to understand the nanoparticle interaction with biological compartments [88].

The interplay between ligand density and ligand intrinsic affinity to its receptor is another important point to be considered. An interesting report evaluated the cellular uptake of liposomes conjugated with scFv antibody fragments that have a wide range of intrinsic affinity (K_D = 264–0.9 nM) [90]. At a high liposomal ligand density (>148 scFv/IL), there was no impact of intrinsic affinities on cellular uptake. At lower ligand densities, there was less uptake of liposomes targeted by the lowest affinity scFv (K_D = 264 nM), but no difference in uptake between liposomes targeted by 15 nM or 0.9 nM scFv. These results suggest that engineering ultrahigh affinity ligands may be unnecessary for optimal nanoparticle targeting and highlight the potential interplay between targeting ligand properties and their density, which should be the subject of further evaluations.

It is well accepted that injected nanoparticles into biological fluids (*e.g.* blood) will allow a significant adsorption of various types of proteins to the surface of the nanoparticle, which significantly changes the nanoparticle's physiochemical properties, identity, biodistribution and tumor homing. This adsorption is known as the formation of protein corona, which is driven by the high surface area of nanoparticles, surface energies, and the presence of various types of proteins in biological fluids that have adsorption affinity to these nanoparticles. The adsorbing proteins (referred as opsonins) includes albumin, apolipoprotiens, components of the complements system and immunoglobulins make it feasible for the mononuclear phagocytic system (MPS),which consists of phagocytic cells such as macrophages residing in spleen, liver and lymph nodes, to recognize the "opsonized" nanoparticles [34,91–93]. Recently, the role of the protein corona and immunoglobulin (IgG) in activation of the complement system and opsonization has been confirmed on clinically used nanomedicines (Feraheme, LipoDox or Onivyde) using human sera [94]. The opsonization of nanoparticles followed by MPS uptake (alternatively named as RES clearance) is determinant to nanoparticle biodistribution and desired pharmacokinetics and results in low tumor homing. Various approaches have been reported to minimize the adsorption of proteins on nanoparticles towards providing nanoparticles with a stealth charter, enhance circulation time and tumor homing. These approaches include surface modification with PEG molecules [95], zwitterionic polymers/ligands [96,97], endogenous cell membranes (*e.g.* coating nanoparticles with plasma membrane of human platelets) [98], pre-coating of nanoparticles with specific protein(s) and employing the protein-protein interaction to recruit targeting proteins during corona formation [99]. Recently. The pre-adsorption of dysopsonic proteins (proteins prevent opsonization) [100,101] and recombinant fusion proteins [102] on nanoparticles showed a significant minimization of protein corona and enhanced tumor targeting. Excellent reviews discussing the formation of protein corona, opsonizations, RES clearance and approaches to avoid these processes are available in the literature [34,92,93,103–109]. Our particular question here is how ligand density and these processes (protein corona formation, opsonization and RES clearance) interplay. While these biological processes have been studied widely for non-targeted nanoparticles, much less is conducted on targeted nanoparticles.

Recent reports showed that the formation of protein corona still applies when nanoparticles bear targeting moieties and indeed this not only occurs for non-targeted counterparts [34,105]. Moreover, it has been reported that the adsorption of proteins can shield and significantly reduce the targeting ability of these nanoparticles. For example, silica nanoparticle targeted with transferrin lost their targeting specificity as sequence of protein corona upon exposure to cell growth media [110]. In another example, polystyrene nanoparticles functionalized with anti-CD63 antibodies *via* chemical attachment completely lose their targeting efficacy in serum or plasma [111]. Mirshafiee et al. reported a decreased targeting efficiencies (94% and 99%) for targeted silica nanoparticles upon Incubation with (10% or 100%) serum, respectively [112]. Varnamkhasti et al. reported a deteriorated targeting capability of aptamer-functionalized nanoparticles upon protein corona formation [113]. In a clear discrepancy to these results, other reports showed minimal or no effect of protein corona on the targeting capability of nanoparticles. For example, the Dawson group reported on reduced, but not "completely obscured", targeting efficiency of single-domain antibody-functionalized nanoparticles in complex bovine and human serum conditions [114]. In another study, the Caruso group reported no determent effect of protein corona formation on antibody-functionalized nanoparticles with preserved surface functionality upon incubation in human serum (note that larger particle were used in this study; polymeric capsule and core-shell particles with diameter of 2 μm) [115]. Interestingly, other reports even report and enhanced specificity of targeted nanoparticle in presence but not in absence of serum protein [116]. The observed conflicting results and the unpredictable targeting outcomes in presence of proteins may be attributed to the use of different types of nanoparticles (size, shape and surface chemistries), targeting ligands (affinity and size) and linker characteristics (length, hydrophilicity and grafting density). Moreover, ligand density, the focus of this review, is expected to be an important parameter which control the interplay between protein corona and cell interaction [105].

Beyond *in vitro* evaluations, evidences of the formation of protein corona on nanoparticles *in vivo* (small animals) are recently reported by various groups [117–121]. Among these few reports, one studied employed targeted nanoparticles (antibody-conjugated liposomes) [117]. In this report it was found that both *in vitro* and *in vivo* formed protein coronas significantly reduce receptor binding and cellular internalization of antibody-conjugated liposomes; however, the *in vivo* corona had wider molecular species, did not coat the liposome surface entirely and did not lead to complete ablation of their targeting capability. Interestingly, a recent study confirmed the formation of protein corona on clinically used PEGylated doxorubicin-encapsulated liposomes (Caelyx) in Human [121]. Authors describe the formed corona as

molecularly richer in composition to its *ex vivo* counterpart (liposomes injected in isolated blood) highlighting the importance of circulation dynamics and presence of circulating cells *in vivo* which cannot stimulated using *in vitro* or *ex vivo* alternatives. Since the evaluation of *in vivo* protein corona formation is relatively recent and unexplored, there is no report evaluating the effect of ligand density on the protein corona *in vivo*. In this context, a recent repot evaluated the protein corona of TAT-functionalized liposomes where it was found that the protein corona thickness increase with TAT density [122]. In this study, it has been found that albumin is the main adsorbing protein and function as dysopsonin that protect targeted liposomes from RES clearance while maintain liposomal targeting capability. However generalization of theses finding should be conservative since TAT is a highly cationic peptide and this character recruit the negatively charged albumin, which may not be the case for other targeting moieties.

It is apparent from the previous discussion that protein corona is a very critical process that nanoparticles experienced *in vitro* and *in vivo* and alter their identity and biological fate and it is unfortunately clear that our understanding of how ligand density of targeted nanoparticles affect the protein corona in biological settings and related sequences need to be enrich though dedicated research in this direction.

6. Chemistry tools to control the density of ligand on nanoparticle

Last but not least, in this section we will discuss chemistry strategies used to control the density of ligands on nanoparticles, whereby we will not go into details to the chemistry of conjugation itself or tools used to preserve the orientation of ligand on nanoparticles. These aspects have been covered by other available reviews [22,27,28,123–127] and are out of the scope of this review. However, at any rate, in order to perform experiments with controlled ligand density obviously the methodology to synthesize such nanoparticles matters.

The typical chemistry approach to vary the number of ligand density on nanoparticles is often based on varying the molar ratio of reactants (ligand:nanoparticle) in the conjugation reaction, followed by purification and surface ligand quantification [54,128,129]. The nanoparticles are first synthesized and prepared for conjugation, then the amount of targeting ligands is varied in the reaction to control the number of ligand conjugated *per* nanoparticle. The simplicity of this approach explains its wide use in reported studies, but it does not allow a precise functionalization with a "predefined" number of ligands *per* nanoparticles. This is important when comparing cellular uptake or *in vivo* behavior for nanoparticles of different size, shape, and other physiochemical properties, where the ligand density or number *per* nanoparticle should be precisely determined.

Another approach employs a pre-prepared "building block-ligand" conjugate that can assemble into targeted nanoparticles. For example Gu et al. prepared a triblock copolymer (PLGA-b-PEG-b-Apt, PLGA is the building block here where the aptamer Apt is the targeting moiety), which was mixed with non-targeted diblock polymer PLGA-b-PEG to form a nanoparticle with PLGA core and a PEG/aptamer shell [54]. The ligand density of the aptamer was varied by mixing a known number of the diblock and triblock polymers as shown in Fig. 7A. However, by varying the ratio between PLGA-b-PEG/ PLGA-b-PEG-b-Apt the nanoparticle size may change, which can add another factor to be considered. Prisner et.al reported tunable aptamer density on gold nanoparticles by *co*-assembly of thiolated PEG and similar polymer with terminal aptamer (SH-PEG_{12} and SH-C_6-PEG_6-aptamer, respectively [130], as shown in Fig. 7B). A similar approach was also employed to control the density of RGD on gold nanoparticles by the co-assembly of SH-PEG and SH-PEG-RGD [131]. In another example, Poon et al. pre-functionalized linear dendritic polymers (LDPs) with folate ligands and the targeted LDP then was assembled in mixed micelle formulations that presented different spatial arrangements of variable sized ligand clusters, and examine the targeting efficacy of these formulations *in vitro* and *in vivo* (Fig. 7C) [88].

Achieving a predefined number of ligands *per* nanoparticle is defiantly not a simple task and it is even more challenging to control the density of ligands at a very low level of surface ligands, such as conjugating a nanoparticle with a single antibody. In this direction, a conjugation chemistry approach has been developed that ensures the functionalization of nanoparticles with discrete low numbers of ligands (exactly one and two ligands per nanoparticle). The described approach depends on coupling nanoparticles bearing terminal functional groups with a linker (PEG molecule) at varied ligand:nanoparticle molar ratio. There is a window of molar ratio (typically at low ligand to nanoparticle ratio) that yields mix of conjugates which includes nanoparticles functionalized with zero, one, two or more ligands. This mix can be then fractionated into discrete bands using gel electrophoresis as function of number of attached ligands *per* nanoparticles [132]. If the ligands bound to a nanoparticle change its overall effective size (or charge) sufficiently, nanoparticles containing different numbers of ligands can be separated based on differential electrophoretic mobility. Nanoparticles can be separated by gel electrophoresis. Extraction of the isolated bands from the gel yields the different conjugates [132]. The described approach further facilitates the modification of colloidal nanoparticles of different materials with a single targeting moiety. This is important when considering the development of targeted nanoparticles for sensing purposes, where a high density of antibody may result in a significant shift from 1:1 interaction and may result in unwanted crosslinking effects and thus might disrupt the quantification outcome. Using this approach gold nanoparticles with different numbers of DNA molecules attached per nanoparticle were sorted and extracted using gel electrophoresis [133,134]. Another group used a similar approach to functionalize silver nanoparticles with discrete numbers of DNA ligands [135]. Furthermore, this approach has been applied to prepare nanoparticles with one or two PEG linker terminated with a functional group for discrete conjugation of targeting moieties (Fig. 8A) [132,136]. For example, discrete functionalization of gold nanoparticles (5 nm) with PEG terminated with amine allowed to prepare trastuzumab-functionalized gold nanoparticles with "exactly" one or two antibody per nanoparticle (Fig. 8A). The "exactly" strictly only holds true assuming 100% conjugation efficiency of antibodies to the amino terminals of PEG and neglecting non-specific antibody adsorption to the nanoparticle surface. With these formulations the difference in cellular binding, uptake and toxicity, as well as *in vivo* tumor targeting and biodistribution as function of the antibody number *per* nanoparticle (one or two) was elucidate, as discussed in the previous sections [78]. This approach was further employed by other groups to functionalize gold nanoparticles with a discrete number of bovine serum albumin (BSA) [137] or monovalent quantum dots with a single antibody [138].

Having outlined chemical approaches to control the ligand density of nanoparticles, one however needs to consider that ligand density may not be a constant parameter. In fact, enzymes may degrade the surface chemistry of nanoparticles [139]. Thus one needs to consider the possibility of *in vitro* and *in vivo* degradation of the ligand shell around nanoparticles, which would reduce the possibility of active targeting [140].

7. Concluding perspective and future directions

One of the major benefits of utilizing nanotechnology in oncology is to achieve a selective accumulation of therapeutics in the desired target and minimum accumulation in other regions. So far, we rely on passive targeting to achieve this task with a satisfactory but limited successes as evident from the presence of few FDA or EMEA approved nanoparticles that home to their targets passively with no targeting moieties [19]. As passive targeting is limited to specific types of cancers and found to be variable according to a recent seminal study in humans [16], active targeting is the next step to boost superior efficacy and safety of nanomedicine. Even though active targeting may have marginal or even no effect on promoting tumor accumulation, it is widely accepted that it alters the microdistribution within tumor promoting active

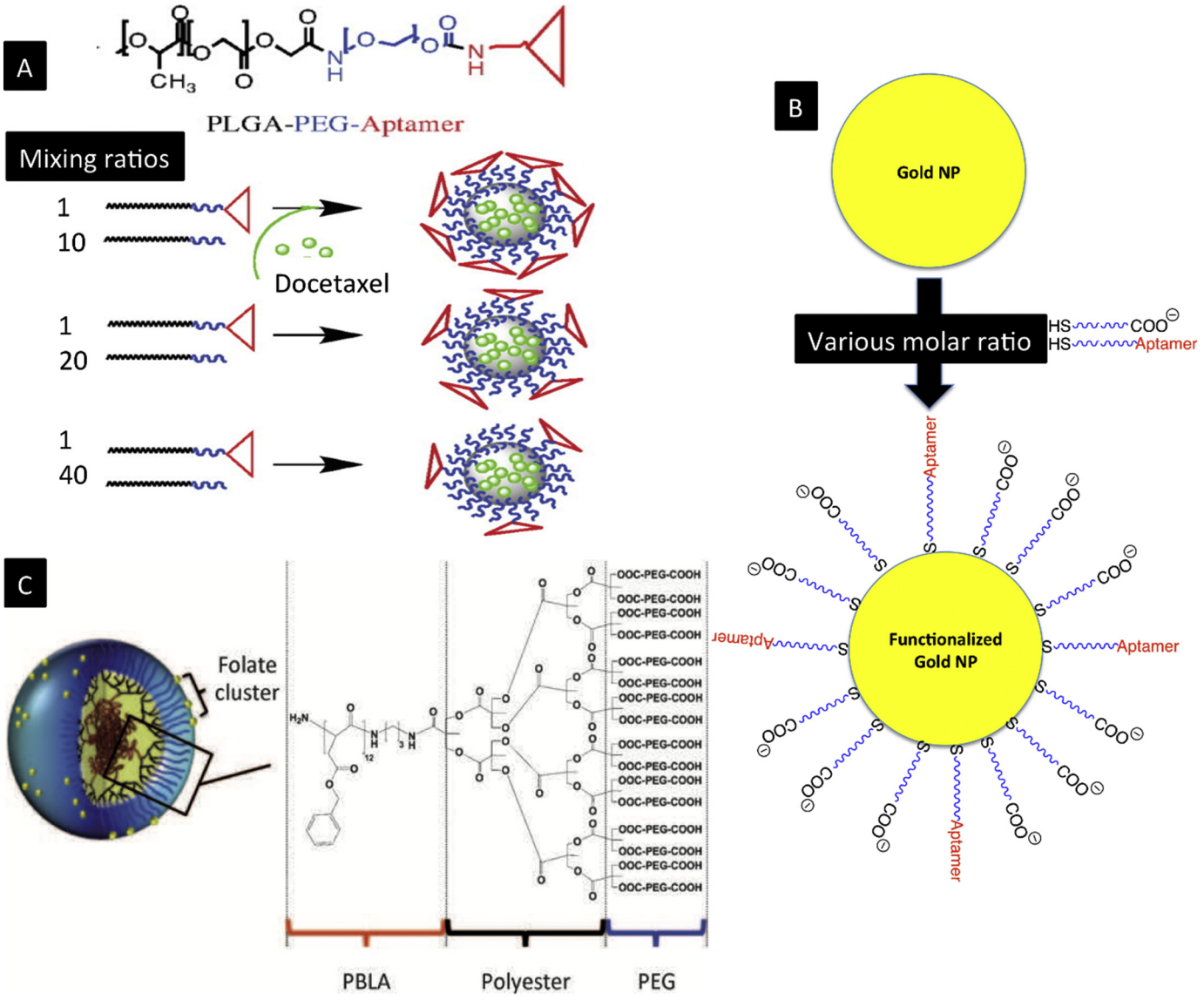

Fig. 7. Examples of controlling the targeting ligand density on the surface of engineered nanoparticles using self-assembly of pre-functionalized targeted building blocks with non-functionalized building blocks in various ratios. A) PLGA-PEG-aptamer was mixed with PLGA-PEG polymers to control the aptamer density on polymeric nanocarriers. B) Thiolated polyethylene glycol was mixed with thiolated polyethylene glycol terminated with aptamer (targeted) to control the aptamer density on gold nanoparticles. C) Detailed chemical structure of the non-folate conjugated linear dendritic polymers and illustration of their self-assembly into "patchy" micelles presenting clusters of folate of variable sizes on the surface of the micelle. PBLA = poly(benzyl-l-aspartic acid). The image in (A) is reused with permission of the National Academy of Sciences from reference [54]. Image in (C) is reused by permission of Wiley from reference [88].

cellular uptake to cancer cells rather than macrophages, which ultimately improves potency of nanotherapeutic. With this in mind, great effort has been assigned to understand the contribution of active targeting and the parameters that control this exciting approach. For example, significant effort has been directed to understand the contribution of added targeted moieties through comparison with non-targeted counterparts both *in vitro* and *in vivo*. In parallel various chemical conjugation approaches have been developed (including oriented and non-classical tools) [141–143] as well as analytical tools [43] to quantify conjugated targeting moieties and to image/quantify nanoparticles in cells/organs. However, precise quantification of the number of targeting ligands per single nanoparticle is still a clear challenge especially for organic nanoparticles. In the case of inorganic nanoparticles such as gold it is easier to quantify the amount of ligand per nanoparticles since total protein analysis can reveal the total number of ligand where ICP-MS analysis can precisely quantify the number of inorganic nanoparticles in the same sample (after a carful isolation of the free unbound ligand) [144]. These quantifications allow for a reliable calculation of the average number of ligand (*e.g.* antibodies) per single nanoparticle. Indeed this is one of the many advantages of using inorganic nanostructures to probe and understand the nano-bio interface [144]. In the case of liposomes, lipid and polymeric nanoparticles, the task of determination of number of ligand per nanoparticle is harder and usually ends up with reporting the number of ligands per weight unit of vehicle (lipid or polymer). In fact the shortage of simple and reliable analytical tools to quantify the number of ligands per liposome is recognized as an important factor that contributes to the slow development of targeted liposomes [145]. Recently, super resolution microscopy with a single molecule localization capability was proven as a powerful tool to map the targeting molecules (antibodies and streptavidin) on the surface of polystyrene nanoparticles and to provide a quantitative estimation of the number and distribution of the attached active ligand with proper orientation [146]. In another report, Van Oijen and co-workers counted functional proteins on the surface of liposomes using single-molecule imaging [145]. These studies opened the way towards multicolour mapping of the

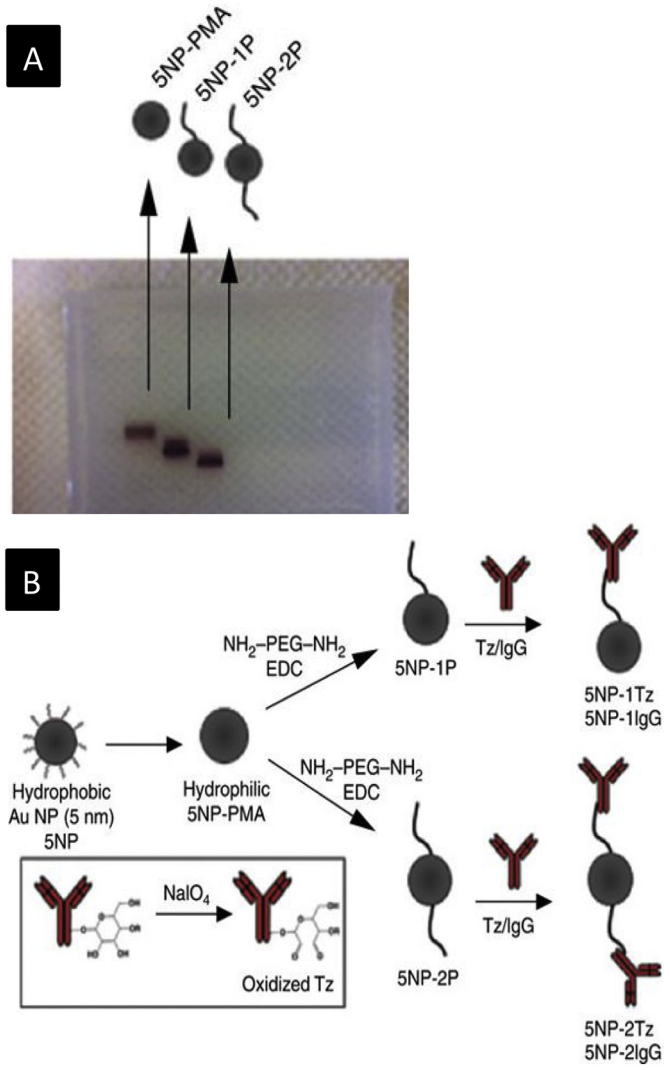

Fig. 8. Precise and discrete bioconjugation. A) Gold nanoparticles (5 nm) with terminal carboxylic acid groups were functionalized with (amine-PEG-amine) at carefully-optimized molar ratio of reactants and then gel electrophoresis was used to separate nanoparticles with exactly 0, 1, or 2 PEGs per nanoparticle (labeled as 5NP-PMA, 5NP-1P and 5NP-2P, respectively). B) These nanoparticles then were coupled to activated antibodies to generate nanoparticles functionalized with only one or two antibodies as shown in the reaction scheme. Graphs in (A) and (B) are reused by permission of Nature publishing Group from reference [78].

functionality of lipid-based drug nanocarriers using super resolution microscopy [147]. However, the need for development of simple and reliable analytical tool to quantify number of ligand per nanoparticles when vehicle is organic in nature (liposome, polymeric, lipid) is a clear need and should be the focus of a dedicated research. In this context, recent development of particle counting techniques [148] is advantageous to determine number of particles followed by determination of number of ligand in same sample to calculate ligand density with reliability. Moreover, analytical methods that can follow up the formation of protein corona in suit and preferably *in vivo* without the need to isolate the nanoparticles and bound proteins to avoid disruption of equilibrium properties and resulting artifacts would be of a great benefit to understand the protein corona of targeted nanoparticles in relevant complex settings [149]. At the other hand, many related details and important questions related to ligand density on nanoparticles still need clearer and evidence-supported answers. These questions, in the context of this review, include: How many targeting ligand should be there on nanoparticle? What is the interplay between targeting ligand density and other ligand-related or nanoparticle-related or disease-related parameters when cellular association or tumor homing is considered? How does the passive and the active targeting interplay depend on ligand density? How does ligand density affect the accumulation of targeted nanoparticles into various types of tumor or tumor stage? How does ligand density alter the diffusional properties of nanoparticles in tumor tissue? How ligand density alters RES clearance of nanoparticles as function of type of ligand (small molecule, antibody fragment, whole antibody, aptamer, *etc*)? How is ligand density altered by possible enzymatic degradation? Answering these questions requires dedicated research and should construct the "road map" for nanoscientists to design efficient and safe targeted nanotherapeutics. In parallel, the development of facile conjugation chemistries that preserve the proper function, orientation and density of targeting ligand with the ability to be scaled up according to good manufacturing practices (GMP) and regulatory guidance is a prerequisite for translational targeted nanomedicine.

Acknowledgements

AMA was supported by an Alexander von Humboldt fellowship. LZ was supported by the Chinese Scholarship Council (CSC). HW, AM, and WJP were funded by the German Research Society (DFG) in the framework of the Cluster of Excellence 'Advanced Imaging of Matter' of the Deutsche Forschungsgemeinschaft (DFG) - EXC 2056 - project ID 390715994. MB acknowledges support by the DFG (CRC 1066-2).

References

[1] B. Pelaz, C. Alexiou, R.A. Alvarez-Puebla, F. Alves, A.M. Andrews, S. Ashraf, L.P. Balogh, L. Ballerini, A. Bestetti, C. Brendel, S. Bosi, M. Carril, W.C.W. Chan, C. Chen, X. Chen, X. Chen, Z. Cheng, D. Cui, J. Du, C. Dullin, A. Escudero, N. Feliu, M. Gao, M. George, Y. Gogotsi, A. Grünweller, Z. Gu, N.J. Halas, N. Hampp, R.K. Hartmann, M.C. Hersam, P. Hunziker, J. Jian, X. Jiang, P. Jungebluth, P. Kadhiresan, K. Kataoka, A. Khademhosseini, J. Kopeček, N.A. Kotov, H.F. Krug, D.S. Lee, C.-M. Lehr, K.W. Leong, X.-J. Liang, M. Ling Lim, L.M. Liz-Marzán, X. Ma, P. Macchiarini, H. Meng, H. Möhwald, P. Mulvaney, A.E. Nel, S. Nie, P. Nordlander, T. Okano, J. Oliveira, T.H. Park, R.M. Penner, M. Prato, V. Puntes, V.M. Rotello, A. Samarakoon, R.E. Schaak, Y. Shen, S. Sjöqvist, A.G. Skirtach, M.G. Soliman, M.M. Stevens, H.-W. Sung, B.Z. Tang, R. Tietze, B.N. Udugama, J.S. VanEpps, T. Weil, P.S. Weiss, I. Willner, Y. Wu, L. Yang, Z. Yue, Q. Zhang, Q. Zhang, X.-E. Zhang, Y. Zhao, X. Zhou, W.J. Parak, Diverse applications of nanomedicine, ACS Nano 11 (2017) 2313–2381.
[2] V. Weissig, T.K. Pettinger, N. Murdock, Nanopharmaceuticals (part 1): products on the market, Int. J. Nanomedicine 9 (2014) 4357–4373.
[3] V. Weissig, D. Guzman-Villanueva, Nanopharmaceuticals (part 2): products in the pipeline, Int. J. Nanomedicine 10 (2015) 1245–1257.
[4] C.L. Ventola, Progress in nanomedicine: approved and investigational nanodrugs, Pharm. Ther. 42 (2017) 742–755.
[5] D. Bobo, K.J. Robinson, J. Islam, K.J. Thurecht, S.R. Corrie, Nanoparticle-based medicines: a review of FDA-approved materials and clinical trials to date, Pharm. Res. 33 (2016) 2373–2387.
[6] Y. Barenholz, Doxil (R) – the first FDA-approved nano-drug: lessons learned, J. Control. Release 160 (2012) 117–134.
[7] H. Maeda, Macromolecular therapeutics in cancer treatment: the EPR effect and beyond, J. Control. Release 164 (2012) 138–144.
[8] S.K. Golombek, J.-N. May, B. Theek, L. Appold, N. Drude, F. Kiessling, T. Lammers, Tumor targeting via EPR: strategies to enhance patient responses, Adv. Drug Deliv. Rev. 130 (2018) 17–38.
[9] A.M. Sofias, M. Dunne, G. Storm, C. Allen, The battle of "nano" paclitaxel, Adv. Drug Deliv. Rev. 122 (2017) 20–30.
[10] E. Miele, G.P. Spinelli, E. Miele, F. Tomao, S. Tomao, Albumin-bound formulation of paclitaxel (Abraxane ABI-007) in the treatment of breast cancer, Int. J. Nanomedicine 4 (2009) 99–105.
[11] L. Zhang, P. Marrano, S. Kumar, M. Leadley, E. Elias, P.S. Thorner, S. Baruchel, Abraxane (nab-paclitaxel) is an active drug in preclinical model of pediatric solid tumors, Clin. Cancer Res. 19 (21) (2013) 5972–5983.
[12] N. Desai, V. Trieu, Z. Yao, L. Louie, S. Ci, A. Yang, C. Tao, T. De, B. Beals, D. Dykes, P. Noker, R. Yao, E. Labao, M. Hawkins, P. Soon-Shiong, Increased antitumor activity, intratumor paclitaxel concentrations, and endothelial cell transport of cremophor-free, albumin-bound paclitaxel, ABI-007, compared with cremophor-based paclitaxel, Clin. Cancer Res. 12 (2006) 1317–1324.
[13] J.P. Barrett, K.A. Vardulaki, C. Conlon, J. Cooke, P. Daza-Ramirez, E.G.V. Evans, P.M. Hawkey, R. Herbrecht, D.I. Marks, J.M. Moraleda, G.R. Park, S.J. Senn, C. Viscoli, A systematic review of the antifungal effectiveness and tolerability of amphotericin B formulations, Clin. Ther. 25 (2003) 1295–1320.

[14] N.K. Jain, V. Mishra, N.K. Mehra, Targeted drug delivery to macrophages, Expert Opin. Drug Deliv. 10 (2013) 353–367.
[15] Y. Pei, Y. Yeo, Drug delivery to macrophages: challenges and opportunities, J. Control. Release 240 (2016) 202–211.
[16] H. Lee, A.F. Shields, B.A. Siegel, K.D. Miller, I. Krop, C.X. Ma, P.M. LoRusso, P.N. Munster, K. Campbell, D.F. Gaddy, S.C. Leonard, E. Geretti, S.J. Blocker, D.B. Kirpotin, V. Moyo, T.J. Wickham, B.S. Hendriks, ^{64}Cu-MM-302 positron emission tomography quantifies variability of enhanced permeability and retention of nanoparticles in relation to treatment response in patients with metastatic breast cancer, Clin. Cancer Res. 23 (2017) 4190–4202.
[17] S. Wilhelm, A.J. Tavares, Q. Dai, S. Ohta, J. Audet, H.F. Dvorak, W.C.W. Chan, Analysis of nanoparticle delivery to tumours, Nat. Rev. Mater. 1 (2016) 16014.
[18] Z. Cheng, A. Al Zaki, J.Z. Hui, V.R. Muzykantov, A. Tsourkas, Multifunctional nanoparticles: cost versus benefit of adding targeting and imaging capabilities, Science 338 (2012) 903–910.
[19] D. Rosenblum, N. Joshi, W. Tao, J.M. Karp, D. Peer, Progress and challenges towards targeted delivery of cancer therapeutics, Nat. Commun. 9 (2018) 1410.
[20] K. Park, Facing the truth about nanotechnology in drug delivery, ACS Nano 7 (2013) 7442–7447.
[21] K.N. Sugahara, T. Teesalu, P.P. Karmali, V.R. Kotamraju, L. Agemy, D.R. Greenwald, E. Ruoslahti, Coadministration of a tumor-penetrating peptide enhances the efficacy of cancer drugs, Science 328 (2010) 1031–1035.
[22] N. Kamaly, Z. Xiao, P.M. Valencia, A.F. Radovic-Moreno, O.C. Farokhzad, Targeted polymeric therapeutic nanoparticles: design, development and clinical translation, Chem. Soc. Rev. 41 (2012) 2971–3010.
[23] M. Nazarenus, Q. Zhang, M.G. Soliman, P. del Pino, B. Pelaz, S. Carregal Romero, J. Rejman, B. Rothen-Ruthishauser, M.J.D. Clift, R. Zellner, G.U. Nienhaus, J.B. Delehanty, I.L. Medintz, W.J. Parak, In vitro interaction of colloidal nanoparticles with mammalian cells: what have we learned thus far? Beilstein J. Nanotechnol. 5 (2014) 1477–1490.
[24] A.J. Sivaram, A. Wardiana, C.B. Howard, S.M. Mahler, K.J. Thurecht, Recent advances in the generation of antibody–nanomaterial conjugates, Adv. Healthc. Mater. 7 (2018) 1700607.
[25] G. Chen, I. Roy, C. Yang, P.N. Prasad, Nanochemistry and nanomedicine for nanoparticle-based diagnostics and therapy, Chem. Rev. 116 (2016) 2826–2885.
[26] R. Toy, L. Bauer, C. Hoimes, K.B. Ghaghada, E. Karathanasis, Targeted nanotechnology for cancer imaging, Adv. Drug Deliv. Rev. 76 (2014) 79–97.
[27] J.-M. Montenegro, V. Grazu, A. Sukhanova, S. Agarwal, J.M.d.l. Fuente, I. Nabiev, A. Greiner, W.J. Parak, Controlled antibody/(bio-) conjugation of inorganic nanoparticles for targeted delivery, Adv. Drug Deliv. Rev. 65 (2013) 677–688.
[28] J. Nam, N. Won, J. Bang, H. Jin, J. Park, S. Jung, S. Jung, Y. Park, S. Kim, Surface engineering of inorganic nanoparticles for imaging and therapy, Adv. Drug Deliv. Rev. 65 (2013) 622–648.
[29] E. Pérez-Herrero, A. Fernández-Medarde, Advanced targeted therapies in cancer: drug nanocarriers, the future of chemotherapy, Eur. J. Pharm. Biopharm. 93 (2015) 52–79.
[30] L.D. Field, J.B. Delehanty, Y. Chen, I.L. Medintz, Peptides for specifically targeting nanoparticles to cellular organelles: Quo Vadis? Acc. Chem. Res. 48 (2015) 1380–1390.
[31] J. Shi, Z. Xiao, N. Kamaly, O.C. Farokhzad, Self-assembled targeted nanoparticles: evolution of technologies and bench to bedside translation, Acc. Chem. Res. 44 (2011) 1123–1134.
[32] H. Koo, M.S. Huh, I.C. Sun, S.H. Yuk, K. Choi, K. Kim, I.C. Kwon, In vivo targeted delivery of nanoparticles for theranosis, Acc. Chem. Res. 44 (2011) 1018–1028.
[33] N. Bertrand, J. Wu, X. Xu, N. Kamaly, O.C. Farokhzad, Cancer nanotechnology: the impact of passive and active targeting in the era of modern cancer biology, Adv. Drug Deliv. Rev. 66 (2014) 2–25.
[34] Q. Dai, N. Bertleff-Zieschang, J.A. Braunger, M. Björnmalm, C. Cortez-Jugo, F. Caruso, Particle targeting in complex biological media, Adv. Healthc. Mater. 7 (2018) 1700575.
[35] Y. Yamauchi, A. Helenius, Virus entry at a glance, J. Cell Sci. 126 (2013) 1289–1295.
[36] T. Heath, R. Fraley, D. Papahdjopoulos, Antibody targeting of liposomes: cell specificity obtained by conjugation of F(ab')2 to vesicle surface, Science 210 (1980) 539–541.
[37] A. Amitai, A.K. Chakraborty, M. Kardar, The low spike density of HIV may have evolved because of the effects of T helper cell depletion on affinity maturation, PLoS Comput. Biol. 14 (2018), e1006408.
[38] G.S. Mohan, L. Ye, W. Li, A. Monteiro, X. Lin, B. Sapkota, B.P. Pollack, R.W. Compans, C. Yang, Less is more: Ebola virus surface glycoprotein expression levels regulate virus production and infectivity, J. Virol. 89 (2015) 1205–1217.
[39] J.S. Klein, P.J. Bjorkman, Few and far between: how HIV may be evading antibody avidity, PLoS Pathog. 6 (2010), e1000908.
[40] E. Bachrach, H. Dreja, Y.-L. Lin, C. Mettling, V. Pinet, P. Corbeau, M. Piechaczyk, Effects of virion surface gp120 density on infection by HIV-1 and viral production by infected cells, Virology 332 (2005) 418–429.
[41] E. Bachrach, M. Marin, M. Pelegrin, G. Karavanas, M. Piechaczyk, Efficient cell infection by Moloney murine leukemia virus-derived particles requires minimal amounts of envelope glycoprotein, J. Virol. 74 (2000) 8480–8486.
[42] R. Sougrat, A. Bartesaghi, J.D. Lifson, A.E. Bennett, J.W. Bess, D.J. Zabransky, S. Subramaniam, Electron tomography of the contact between T cells and SIV/HIV-1: implications for viral entry, PLoS Pathog. 3 (2007), e63.
[43] A.M. Smith, K.A. Johnston, S.E. Crawford, L.E. Marbella, J.E. Millstone, Ligand density quantification on colloidal inorganic nanoparticles, Analyst 142 (2017) 11–29.
[44] P. Zhu, E. Chertova, J. Bess, J.D. Lifson, L.O. Arthur, J. Liu, K.A. Taylor, K.H. Roux, Electron tomography analysis of envelope glycoprotein trimers on HIV and simian immunodeficiency virus virions, Proc. Natl. Acad. Sci. 100 (2003) 15812–15817.
[45] V.M. Prasad, A.S. Miller, T. Klose, D. Sirohi, G. Buda, W. Jiang, R.J. Kuhn, M.G. Rossmann, Structure of the immature Zika virus at 9 Å resolution, Nat. Struct. Mol. Biol. 24 (2017) 184.
[46] K. Grünewald, P. Desai, D.C. Winkler, J.B. Heymann, D.M. Belnap, W. Baumeister, A.C. Steven, Three-dimensional structure of herpes simplex virus from cryo-electron tomography, Science 302 (2003) 1396–1398.
[47] M. Yamaguchi, R. Danev, K. Nishiyama, K. Sugawara, K. Nagayama, Zernike phase contrast electron microscopy of ice-embedded influenza A virus, J. Struct. Biol. 162 (2008) 271–276.
[48] X. Zhang, J. Sheng, S.K. Austin, T.E. Hoornweg, J.M. Smit, R.J. Kuhn, M.S. Diamond, M.G. Rossmann, Structure of acidic pH dengue virus showing the fusogenic glycoprotein trimers, J. Virol. 89 (2015) 743–750.
[49] A. Merz, G. Long, M.-S. Hiet, B. Brügger, P. Chlanda, P. Andre, F. Wieland, J. Krijnse-Locker, R. Bartenschlager, Biochemical and morphological properties of hepatitis C virus particles and determination of their lipidome, J. Biol. Chem. 286 (2011) 3018–3032.
[50] J.H. Lee, A. Sahu, C. Jang, G. Tae, The effect of ligand density on in vivo tumor targeting of nanographene oxide, J. Control. Release 209 (2015) 219–228.
[51] K.G. Reuter, J.L. Perry, D. Kim, J.C. Luft, R. Liu, J.M. DeSimone, Targeted PRINT hydrogels: the role of nanoparticle size and ligand density on cell association, biodistribution, and tumor accumulation, Nano Lett. 15 (2015) 6371–6378.
[52] D.R. Elias, A. Poloukhtine, V. Popik, A. Tsourkas, Effect of ligand density, receptor density, and nanoparticle size on cell targeting, Nanomedicine 9 (2013) 194–201.
[53] J. Li, Y. Chen, N. Kawazoe, G. Chen, Ligand density-dependent influence of arginine–glycine–aspartate functionalized gold nanoparticles on osteogenic and adipogenic differentiation of mesenchymal stem cells, Nano Res. 11 (2018) 1247–1261.
[54] F. Gu, L. Zhang, B.A. Teply, N. Mann, A. Wang, A.F. Radovic-Moreno, R. Langer, O.C. Farokhzad, Precise engineering of targeted nanoparticles by using self-assembled biointegrated block copolymers, Proc. Natl. Acad. Sci. U. S. A. 105 (2008) 2586–2591.
[55] P. Zhu, J. Liu, J. Bess Jr., E. Chertova, J.D. Lifson, H. Grisé, G.A. Ofek, K.A. Taylor, K.H. Roux, Distribution and three-dimensional structure of AIDS virus envelope spikes, Nature 441 (2006) 847.
[56] X. Zhang, A. Patel, C.C. Celma, X. Yu, P. Roy, Z.H. Zhou, Atomic model of a nonenveloped virus reveals pH sensors for a coordinated process of cell entry, Nat. Struct. Mol. Biol. 23 (2015) 74.
[57] D.A. Giljohann, D.S. Seferos, P.C. Patel, J.E. Millstone, N.L. Rosi, C.A. Mirkin, Oligonucleotide loading determines cellular uptake of DNA-modified gold nanoparticles, Nano Lett. 7 (2007) 3818–3821.
[58] H.-m. Ding, Y.-q. Ma, Role of physicochemical properties of coating ligands in receptor-mediated endocytosis of nanoparticles, Biomaterials 33 (2012) 5798–5802.
[59] A. Bandyopadhyay, R.L. Fine, S. Demento, L.K. Bockenstedt, T.M. Fahmy, The impact of nanoparticle ligand density on dendritic-cell targeted vaccines, Biomaterials 32 (2011) 3094–3105.
[60] M. Semmling, O. Kreft, A. Muñoz Javier, G.B. Sukhorukov, J. Käs, W.J. Parak, A novel flow-cytometry-based assay for cellular uptake studies of polyelectrolyte microcapsules, Small 4 (2008) 1763–1768.
[61] K.B. Ghaghada, J. Saul, J.V. Natarajan, R.V. Bellamkonda, A.V. Annapragada, Folate targeting of drug carriers: a mathematical model, J. Control. Release 104 (2005) 113–128.
[62] J.A. Reddy, C. Abburi, H. Hofland, S.J. Howard, I. Vlahov, P. Wils, C.P. Leamon, Folate-targeted, cationic liposome-mediated gene transfer into disseminated peritoneal tumors, Gene Ther. 9 (2002) 1542.
[63] M. Barz, F. Canal, K. Koynov, R. Zentel, M.J. Vicent, Synthesis and in vitro evaluation of defined HPMA folate conjugates: influence of aggregation on folate receptor (FR) mediated cellular uptake, Biomacromolecules 11 (2010) 2274–2282.
[64] J. Wang, S. Tian, R.A. Petros, M.E. Napier, J.M. DeSimone, The complex role of multivalency in nanoparticles targeting the transferrin receptor for cancer therapies, J. Am. Chem. Soc. 132 (2010) 11306–11313.
[65] P.S. Tang, S. Sathiamoorthy, L.C. Lustig, R. Ponzielli, I. Inamoto, L.Z. Penn, J.A. Shin, W.C.W. Chan, The role of ligand density and size in mediating quantum dot nuclear transport, Small 10 (2014) 4182–4192.
[66] C. Dalal, A. Saha, N.R. Jana, Nanoparticle multivalency directed shifting of cellular uptake mechanism, J. Phys. Chem. C 120 (2016) 6778–6786.
[67] I.A. Khalil, K. Kogure, S. Futaki, H. Harashima, High density of octaarginine stimulates macropinocytosis leading to efficient intracellular trafficking for gene expression, J. Biol. Chem. 281 (2006) 3544–3551.
[68] A. Akhter, Y. Hayashi, Y. Sakurai, N. Ohga, K. Hida, H. Harashima, Ligand density at the surface of a nanoparticle and different uptake mechanism: two important factors for successful siRNA delivery to liver endothelial cells, Int. J. Pharm. 475 (2014) 227–237.
[69] X. Song, R. Li, H. Deng, Y. Li, Y. Cui, H. Zhang, W. Dai, B. He, Y. Zheng, X. Wang, Q. Zhang, Receptor mediated transcytosis in biological barrier: the influence of receptor character and their ligand density on the transmembrane pathway of active-targeting nanocarriers, Biomaterials 180 (2018) 78–90.
[70] S. Barua, S. Mitragotri, Challenges associated with penetration of nanoparticles across cell and tissue barriers: a review of current status and future prospects, Nano Today 9 (2014) 223–243.
[71] A.T. Florence, "Targeting" nanoparticles: the constraints of physical laws and physical barriers, J. Control. Release 164 (2012) 115–124.
[72] I.K. Kwon, S.C. Lee, B. Han, K. Park, Analysis on the current status of targeted drug delivery to tumors, J. Control. Release 164 (2012) 108–114.

[73] S. Steichen, M. Caldorera-Moore, N. Peppas, A review of current nanoparticle and targeting moieties for the delivery of cancer therapeutics, Eur. J. Pharm. Sci. 48 (2013) 416–427.
[74] R. Toy, K. Roy, Engineering nanoparticles to overcome barriers to immunotherapy, Bioeng. Transl. Med. 1 (2016) 47–62.
[75] S. Mitragotri, P.A. Burke, R. Langer, Overcoming the challenges in administering biopharmaceuticals: formulation and delivery strategies, Nat. Rev. Drug Discov. 13 (2014) 655–672.
[76] D.E. Owens 3rd, N.A. Peppas, Opsonization, biodistribution, and pharmacokinetics of polymeric nanoparticles, Int. J. Pharm. 307 (2006) 93–102.
[77] A.J. Shoffstall, L.M. Everhart, M.E. Varley, E.S. Soehnlen, A.M. Shick, J.S. Ustin, E.B. Lavik, Tuning ligand density on intravenous hemostatic nanoparticles dramatically increases survival following blunt trauma, Biomacromolecules 14 (2013) 2790–2797.
[78] M. Colombo, L. Fiandra, G. Alessio, S. Mazzucchelli, M. Nebuloni, C.D. Palma, K. Kantner, B. Pelaz, R. Rotem, F. Corsi, W.J. Parak, D. Prosperi, Tumour homing and therapeutic effect of colloidal nanoparticles depend on the number of attached antibodies, Nat. Commun. 7 (2016) 13818.
[79] S. Barua, J.W. Yoo, P. Kolhar, A. Wakankar, Y.R. Gokarn, S. Mitragotri, Particle shape enhances specificity of antibody-displaying nanoparticles, Proc. Natl. Acad. Sci. U. S. A. 110 (2013) 3270–3275.
[80] J. Liu, G.E.R. Weller, B. Zern, P.S. Ayyaswamy, D.M. Eckmann, V.R. Muzykantov, R. Radhakrishnan, Computational model for nanocarrier binding to endothelium validated using in vivo, in vitro, and atomic force microscopy experiments, Proc. Natl. Acad. Sci. 107 (2010) 16530–16535.
[81] P. Decuzzi, M. Ferrari, The adhesive strength of non-spherical particles mediated by specific interactions, Biomaterials 27 (2006) 5307–5314.
[82] P. Decuzzi, M. Ferrari, The receptor-mediated endocytosis of nonspherical particles, Biophys. J. 94 (2008) 3790–3797.
[83] L. Li, Y. Zhang, J. Wang, Effects of ligand distribution on receptor-diffusion-mediated cellular uptake of nanoparticles, R. Soc. Open Sci. 4 (2017).
[84] H. Yuan, J. Li, G. Bao, S. Zhang, Variable nanoparticle-cell adhesion strength regulates cellular uptake, Phys. Rev. Lett. 105 (2010) 138101.
[85] H. Yuan, S. Zhang, Effects of particle size and ligand density on the kinetics of receptor-mediated endocytosis of nanoparticles, Appl. Phys. Lett. 96 (2010), 033704.
[86] S. Zhang, H. Gao, G. Bao, Physical principles of nanoparticle cellular endocytosis, ACS Nano 9 (2015) 8655–8671.
[87] K.C. Tjandra, P. Thordarson, Multivalency in Drug Delivery-When Is It Too Much of a Good Thing? Bioconjug Chem. 30 (3) (2019 Mar 20) 503–514, https://doi.org/10.1021/acs.bioconjchem.8b00804.
[88] Z. Poon, S. Chen, A.C. Engler, H.-i. Lee, E. Atas, G. von Maltzahn, S.N. Bhatia, P.T. Hammond, Ligand-clustered "patchy" nanoparticles for modulated cellular uptake and in vivo tumor targeting, Angew. Chem. Int. Ed. 49 (2010) 7266–7270.
[89] E. Moradi, D. Vllasaliu, M. Garnett, F. Falcone, S. Stolnik, Ligand density and clustering effects on endocytosis of folate modified nanoparticles, RSC Adv. 2 (2012) 3025–3033.
[90] Y. Zhou, D.C. Drummond, H. Zou, M.E. Hayes, G.P. Adams, D.B. Kirpotin, J.D. Marks, Impact of single-chain Fv antibody fragment affinity on nanoparticle targeting of epidermal growth factor receptor-expressing tumor cells, J. Mol. Biol. 371 (2007) 934–947.
[91] E. Blanco, H. Shen, M. Ferrari, Principles of nanoparticle design for overcoming biological barriers to drug delivery, Nat. Biotechnol. 33 (2015) 941–951.
[92] S. Zanganeh, R. Spitler, M. Erfanzadeh, A.M. Alkilany, M. Mahmoudi, Protein corona: opportunities and challenges, Int. J. Biochem. Cell Biol. 75 (2016) 143–147.
[93] S. Behzadi, V. Serpooshan, W. Tao, M.A. Hamaly, M.Y. Alkawareek, E.C. Dreaden, D. Brown, A.M. Alkilany, O.C. Farokhzad, M. Mahmoudi, Cellular uptake of nanoparticles: journey inside the cell, Chem. Soc. Rev. 46 (2017) 4218–4244.
[94] V.P. Vu, G.B. Gifford, F. Chen, H. Benasutti, G. Wang, E.V. Groman, R. Scheinman, L. Saba, S.M. Moghimi, D. Simberg, Immunoglobulin deposition on biomolecule corona determines complement opsonization efficiency of preclinical and clinical nanoparticles, Nat. Nanotechnol. 14 (3) (2019) 260–268.
[95] J.S. Suk, Q. Xu, N. Kim, J. Hanes, L.M. Ensign, PEGylation as a strategy for improving nanoparticle-based drug and gene delivery, Adv. Drug Deliv. Rev. 99 (2016) 28–51.
[96] D.F. Moyano, K. Saha, G. Prakash, B. Yan, H. Kong, M. Yazdani, V.M. Rotello, Fabrication of corona-free nanoparticles with tunable hydrophobicity, ACS Nano 8 (2014) 6748–6755.
[97] J. Zhao, Z. Qin, J. Wu, L. Li, Q. Jin, J. Ji, Zwitterionic stealth peptide-protected gold nanoparticles enable long circulation without the accelerated blood clearance phenomenon, Biomater. Sci. 6 (2018) 200–206.
[98] C.-M.J. Hu, R.H. Fang, K.-C. Wang, B.T. Luk, S. Thamphiwatana, D. Dehaini, P. Nguyen, P. Angsantikul, C.H. Wen, A.V. Kroll, C. Carpenter, M. Ramesh, V. Qu, S.H. Patel, J. Zhu, W. Shi, F.M. Hofman, T.C. Chen, W. Gao, K. Zhang, S. Chien, L. Zhang, Nanoparticle biointerfacing by platelet membrane cloaking, Nature 526 (2015) 118.
[99] V. Mirshafiee, R. Kim, S. Park, M. Mahmoudi, M.L. Kraft, Impact of protein precoating on the protein corona composition and nanoparticle cellular uptake, Biomaterials 75 (2016) 295–304.
[100] D.R. Absolom, [13] Opsonins and dysopsonins: An overview, Methods in Enzymology, Academic Press 1986, pp. 281–318.
[101] T. Takeuchi, Y. Kitayama, R. Sasao, T. Yamada, K. Toh, Y. Matsumoto, K. Kataoka, Molecularly imprinted Nanogels acquire stealth in situ by cloaking themselves with native dysopsonic proteins, Angew. Chem. Int. Ed. 56 (2017) 7088–7092.
[102] J.Y. Oh, H.S. Kim, L. Palanikumar, E.M. Go, B. Jana, S.A. Park, H.Y. Kim, K. Kim, J.K. Seo, S.K. Kwak, C. Kim, S. Kang, J.-H. Ryu, Cloaking nanoparticles with protein corona shield for targeted drug delivery, Nat. Commun. 9 (2018) 4548.
[103] P. Aggarwal, J.B. Hall, C.B. McLeland, M.A. Dobrovolskaia, S.E. McNeil, Nanoparticle interaction with plasma proteins as it relates to particle biodistribution, biocompatibility and therapeutic efficacy, Adv. Drug Deliv. Rev. 61 (2009) 428–437.
[104] M. Mahmoudi, N. Bertrand, H. Zope, O.C. Farokhzad, Emerging understanding of the protein corona at the nano-bio interfaces, Nano Today 11 (2016) 817–832.
[105] W. Xiao, H. Gao, The impact of protein corona on the behavior and targeting capability of nanoparticle-based delivery system, Int. J. Pharm. 552 (2018) 328–339.
[106] G. Caracciolo, O.C. Farokhzad, M. Mahmoudi, Biological identity of nanoparticles in vivo: clinical implications of the protein corona, Trends Biotechnol. 35 (2017) 257–264.
[107] H. Gao, Q. He, The interaction of nanoparticles with plasma proteins and the consequent influence on nanoparticles behavior, Expert Opin. Drug Deliv. 11 (2014) 409–420.
[108] I. Lynch, T. Cedervall, M. Lundqvist, C. Cabaleiro-Lago, S. Linse, K.A. Dawson, The nanoparticle - protein complex as a biological entity; a complex fluids and surface science challenge for the 21st century, Adv. Colloid Interf. Sci. 134-35 (2007) 167–174.
[109] P. del Pino, B. Pelaz, Q. Zhang, P. Maffre, G.U. Nienhaus, W.J. Parak, Protein corona formation around nanoparticles-from the past to the future, Mater. Horiz. 1 (2014) 301–313.
[110] A. Salvati, A.S. Pitek, M.P. Monopoli, K. Prapainop, F.B. Bombelli, D.R. Hristov, P.M. Kelly, C. Aberg, E. Mahon, K.A. Dawson, Transferrin-functionalized nanoparticles lose their targeting capabilities when a biomolecule corona adsorbs on the surface, Nat. Nanotechnol. 8 (2013) 137–143.
[111] M. Tonigold, J. Simon, D. Estupiñán, M. Kokkinopoulou, J. Reinholz, U. Kintzel, A. Kaltbeitzel, P. Renz, M.P. Domogalla, K. Steinbrink, I. Lieberwirth, D. Crespy, K. Landfester, V. Mailänder, Pre-adsorption of antibodies enables targeting of nanocarriers despite a biomolecular corona, Nat. Nanotechnol. 13 (2018) 862.
[112] V. Mirshafiee, M. Mahmoudi, K. Lou, J. Cheng, M.L. Kraft, Protein corona significantly reduces active targeting yield, Chem. Commun. 49 (2013) 2557–2559.
[113] B.S. Varnamkhasti, H. Hosseinzadeh, M. Azhdarzadeh, S.Y. Vafaei, M. Esfandyari-Manesh, Z.H. Mirzaie, M. Amini, S.N. Ostad, F. Atyabi, R. Dinarvand, Protein corona hampers targeting potential of MUC1 aptamer functionalized SN-38 core–shell nanoparticles, Int. J. Pharm. 494 (2015) 430–444.
[114] K. Zarschler, K. Prapainop, E. Mahon, L. Rocks, M. Bramini, P.M. Kelly, H. Stephan, K.A. Dawson, Diagnostic nanoparticle targeting of the EGF-receptor in complex biological conditions using single-domain antibodies, Nanoscale 6 (2014) 6046–6056.
[115] Q. Dai, Y. Yan, C.-S. Ang, K. Kempe, M.M.J. Kamphuis, S.J. Dodds, F. Caruso, Monoclonal antibody-functionalized multilayered particles: targeting cancer cells in the presence of protein coronas, ACS Nano 9 (2015) 2876–2885.
[116] Y. Ju, Q. Dai, J. Cui, Y. Dai, T. Suma, J.J. Richardson, F. Caruso, Improving targeting of metal–phenolic capsules by the presence of protein coronas, ACS Appl. Mater. Interfaces 8 (2016) 22914–22922.
[117] M. Hadjidemetriou, Z. Al-Ahmady, M. Mazza, R.F. Collins, K. Dawson, K. Kostarelos, In vivo biomolecule corona around blood-circulating, clinically used and antibody-targeted lipid bilayer nanoscale vesicles, ACS Nano 9 (2015) 8142–8156.
[118] M. Hadjidemetriou, Z. Al-Ahmady, K. Kostarelos, Time-evolution of in vivo protein corona onto blood-circulating PEGylated liposomal doxorubicin (DOXIL) nanoparticles, Nanoscale 8 (2016) 6948–6957.
[119] Z.S. Al-Ahmady, M. Hadjidemetriou, J. Gubbins, K. Kostarelos, Formation of protein corona in vivo affects drug release from temperature-sensitive liposomes, J. Control. Release 276 (2018) 157–167.
[120] A. Amici, G. Caracciolo, L. Digiacomo, V. Gambini, C. Marchini, M. Tilio, A.L. Capriotti, V. Colapicchioni, R. Matassa, G. Familiari, S. Palchetti, D. Pozzi, M. Mahmoudi, A. Laganà, In vivo protein corona patterns of lipid nanoparticles, RSC Adv. 7 (2017) 1137–1145.
[121] M. Hadjidemetriou, S. McAdam, G. Garner, C. Thackeray, D. Knight, D. Smith, Z. Al-Ahmady, M. Mazza, J. Rogan, A. Clamp, K. Kostarelos, The human in vivo biomolecule corona onto PEGylated liposomes: a proof-of-concept clinical study, Adv. Mater. 31 (2019) 1803335.
[122] M. Amin, M. Bagheri, M. Mansourian, M.R. Jaafari, T.L. Ten Hagen, Regulation of in vivo behavior of TAT-modified liposome by associated protein corona and avidity to tumor cells, Int. J. Nanomedicine 13 (2018) 7441–7455.
[123] N.H. Abd Ellah, S.A. Abouelmagd, Surface functionalization of polymeric nanoparticles for tumor drug delivery: approaches and challenges, Expert Opin. Drug Deliv. 14 (2017) 201–214.
[124] J.-H. Oh, D.H. Park, J.H. Joo, J.-S. Lee, Recent advances in chemical functionalization of nanoparticles with biomolecules for analytical applications, Anal. Bioanal. Chem. 407 (2015) 8627–8645.
[125] R. Mout, D.F. Moyano, S. Rana, V.M. Rotello, Surface functionalization of nanoparticles for nanomedicine, Chem. Soc. Rev. 41 (2012) 2539–2544.
[126] J.R. McCarthy, R. Weissleder, Multifunctional magnetic nanoparticles for targeted imaging and therapy, Adv. Drug Deliv. Rev. 60 (2008) 1241.
[127] F.M. Veronese, M. Morpurgo, Bioconjugation in pharmaceutical chemistry, Il Farmaco 54 (1999) 497–516.
[128] H. Lee, T.W. Odom, Controlling ligand density on nanoparticles as a means to enhance biological activity, Nanomedicine 10 (2015) 177–180.
[129] D.R. Hristov, L. Rocks, P.M. Kelly, S.S. Thomas, A.S. Pitek, P. Verderio, E. Mahon, K.A. Dawson, Tuning of nanoparticle biological functionality through controlled surface chemistry and characterisation at the bioconjugated nanoparticle surface, Sci. Rep. 5 (2015) 17040.
[130] L. Prisner, N. Bohn, U. Hahn, A. Mews, Size dependent targeted delivery of gold nanoparticles modified with the IL-6R-specific aptamer AIR-3A to IL-6R-carrying cells, Nanoscale 9 (2017) 14486–14498.

[131] G. Su, H. Jiang, B. Xu, Y. Yu, X. Chen, Effects of protein corona on active and passive targeting of cyclic RGD peptide-functionalized PEGylation nanoparticles, Mol. Pharm. 15 (2018) 5019–5030.
[132] R.A. Sperling, T. Pellegrino, J.K. Li, W.H. Chang, W.J. Parak, Electrophoretic separation of nanoparticles with a discrete number of functional groups, Adv. Funct. Mater. 16 (2006) 943–948.
[133] S.A. Claridge, H.W. Liang, S.R. Basu, J.M.J. Frechet, A.P. Alivisatos, Isolation of discrete nanoparticle−DNA conjugates for plasmonic applications, Nano Lett. 8 (2008) 1202–1206.
[134] D. Zanchet, C.M. Micheel, W.J. Parak, D. Gerion, A.P. Alivisatos, Electrophoretic isolation of discrete Au nanocrystal/DNA conjugates, Nano Lett. 1 (2001) 32–35.
[135] Y. Zheng, Y. Li, Z. Deng, Silver nanoparticle–DNA bionanoconjugates bearing a discrete number of DNA ligands, Chem. Commun. 48 (2012) 6160–6162.
[136] R.A. Sperling, W.J. Parak, Surface modification, functionalization and bioconjugation of colloidal inorganic nanoparticles, Philos. Trans. A Math. Phys. Eng. Sci. 368 (2010) 1333–1383.
[137] R. Zhong, Y. Liu, P. Zhang, J. Liu, G. Zhao, F. Zhang, Discrete nanoparticle-BSA conjugates manipulated by hydrophobic interaction, ACS Appl. Mater. Interfaces 6 (2014) 19465–19470.
[138] H.Y. Liu, X. Gao, Engineering monovalent quantum dot−antibody bioconjugates with a hybrid gel system, Bioconjug. Chem. 22 (2011) 510–517.
[139] M. Chanana, P. Rivera Gil, M.A. Correa-Duarte, W.J. Parak, L.M. Liz-Marzán, Physicochemical properties of protein-coated gold nanoparticles in biological fluids and cells before and after proteolytic digestion, Angew. Chem. Int. Ed. 52 (2013) 4179–4183.
[140] N. Feliu, D. Docter, M. Heine, P. Del Pino, S. Ashraf, J. Kolosnjaj-Tabi, P. Macchiarini, P. Nielsen, D. Alloyeau, F. Gazeau, R.H. Stauber, W.J. Parak, In vivo degeneration and the fate of inorganic nanoparticles, Chem. Soc. Rev. 45 (2016) 2440–2457.
[141] S. Avvakumova, M. Colombo, E. Galbiati, S. Mazzucchelli, R. Rotem, D. Prosperi, Chapter 6 – Bioengineered approaches for site orientation of peptide-based ligands of nanomaterials, in: B. Sarmento, J. das Neves (Eds.), Biomedical Applications of Functionalized Nanomaterials, Elsevier 2018, pp. 139–169.
[142] A.A. Karyakin, G.V. Presnova, M.Y. Rubtsova, A.M. Egorov, Oriented immobilization of antibodies onto the gold surfaces via their native thiol groups, Anal. Chem. 72 (2000) 3805–3811.
[143] C.-W. Tsai, S.-L. Jheng, W.-Y. Chen, R.-C. Ruaan, Strategy of fc-recognizable peptide ligand design for oriented immobilization of antibody, Anal. Chem. 86 (2014) 2931–2938.
[144] A.M. Alkilany, S.E. Lohse, C.J. Murphy, The gold standard: gold nanoparticle libraries to understand the nano-bio Interface, Acc. Chem. Res. 46 (2013) 650–661.
[145] L. Belfiore, L.M. Spenkelink, M. Ranson, A.M. van Oijen, K.L. Vine, Quantification of ligand density and stoichiometry on the surface of liposomes using single-molecule fluorescence imaging, J. Control. Release 278 (2018) 80–86.
[146] P. Delcanale, B. Miret-Ontiveros, M. Arista-Romero, S. Pujals, L. Albertazzi, Nanoscale mapping functional sites on nanoparticles by points accumulation for imaging in nanoscale topography (PAINT), ACS Nano 12 (2018) 7629–7637.
[147] S. Pujals, N. Feiner-Gracia, P. Delcanale, I. Voets, L. Albertazzi, Super-resolution microscopy as a powerful tool to study complex synthetic materials, Nat. Rev. Chem. 3 (2019) 68–84.
[148] J. Shang, X. Gao, Nanoparticle counting: towards accurate determination of the molar concentration, Chem. Soc. Rev. 43 (2014) 7267–7278.
[149] M. Carril, D. Padro, P.d. Pino, C. Carrillo-Carrion, M. Gallego, W.J. Parak, In situ detection of the protein corona in complex environments, Nat. Commun. 8 (2017) 1542.